"DETECTION AND CHARACTERISATION OF RENAL MASSES BY MULTIDETECTOR COMPUTED TOMOGRAPHY."

By

Dr. NANDISH H R M.B.B.S

Dissertation submitted to

BLDE UNIVERSITY,VIJAYAPUR. KARNATAKA.

IN PARTIAL FULFILLMENT OF THE REQUIREMENTS FOR THE DEGREE OF

MASTER OF DEGREE

IN

RADIO-DIAGNOSIS & IMAGING

Under the guidance of

Dr. B R DHAMANGOANKAR M.B.B.S M.D.,D.M. R.D.

PROFESSOR,

DEPARTMENT OF RADIO-DIAGNOSIS & IMAGING

BLDEU'S

SHRI B. M. PATIL MEDICAL COLLEGE,

HOSPITAL & RESEARCH CENTRE.

VIJAYAPUR – 586103

2016-17

I

B.L.D.E. UNIVERSITY'S

SHRI B. M. PATIL MEDICAL COLLEGE, HOSPITAL

& RESEARCH CENTRE, VIJAYAPUR

DECLARATION BY THE CANDIDATE

I, **Dr. NANDISH H R** hereby declare that this dissertation entitled "**DETECTION AND CHARACTERISATION OF RENAL MASSES BY MULTIDETECTOR COMPUTED TOMOGRAPHY**"is a bonafide and genuine research work carried out by me under the guidance of **Dr. B R DHAMANGOANKAR M.D.,** Professor, Department of Radiodiagnosis, B.L.D.E.U's Shri B. M. Patil Medical College Hospital and Research Centre, Vijayapur.

Date: **Dr. NANDISH H R**

Place: Vijayapur   Post Graduate Student,

Department of Radiodiagnosis,

B.L.D.E.U's Shri B. M. Patil Medical

College, Hospital & Research Centre, Vijayapur

B.L.D.E. UNIVERSITY'S

SHRI B. M. PATIL MEDICAL COLLEGE, HOSPITAL

& RESEARCH CENTRE, VIJAYAPUR

CERTIFICATE BY THE GUIDE

This to certify that the dissertation entitled **"DETECTION AND CHARACTERISATION OF RENAL MASSES BY MULTIDETECTOR COMPUTED TOMOGRAPHY"** is a bonafide research work done by **Dr. NANDISH H R**, under my overall supervision and guidance, in partial fulfillment of the requirements for the degree of M. D. in Radiodiagnosis.

Date: **Dr. Dr. B R DHAMANGOANKAR**

Place: Vijayapur   Professor,

                                     Department of Radiodiagnosis,

                                     B.L.D.E.U's Shri B. M. Patil Medical College,

                                     Hospital & Research Centre, Vijayapur

B.L.D.E. UNIVERSITY'S

SHRI B. M. PATIL MEDICAL COLLEGE, HOSPITAL

& RESEARCH CENTRE, VIJAYAPUR

ENDORSEMENT BY THE HEAD OF DEPARTMENT

This to certify that the dissertation entitled **"DETECTION AND CHARACTERISATION OF RENAL MASSES BY MULTIDETECTOR COMPUTED TOMOGRAPHY"** is a bonafide research work done by **Dr.NANDISH H R** under the guidance of **Dr. B R DHAMANGOANKAR** M.D.,Professor, Department of Radiodiagnosis at B.L.D.E.U's Shri B. M. Patil Medical College Hospital and Research Centre, Vijayapur.

Date: **DR. BHUSHAN N. LAKHKAR**M.D.

Place: Vijayapur   Professor & HOD,

                                                     Department of Radiodiagnosis,

                                                     B.L.D.E.U's Shri B. M. Patil Medical College,

                                                     Hospital & Research Centre, Vijayapur

B.L.D.E. UNIVERSITY'S

SHRI B. M. PATIL MEDICAL COLLEGE, HOSPITAL

& RESEARCH CENTRE, VIJAYAPUR

ENDORSEMENT BY THE PRINCIPAL

This to certify that the dissertation entitled **"DETECTION AND CHARACTERISATION OF RENAL MASSES BY MULTIDETECTOR COMPUTED TOMOGRAPHY "**is a bonafide research work done by **Dr.NANDISH H R,** under the guidance of **Dr. B R DHAMANGOANKAR M.D.,** Professor, Department of Radiodiagnosis at B.L.D.E.U's Shri B. M. Patil Medical College Hospital and Research Centre, Vijayapur.

Date**:**   **Dr. S. P. GUGGARIGOUDAR** MS

Place: Vijayapur.   Principal,

                                                  B.L.D.E.U'sShri B. M. Patil Medical College,

                                                  Hospital & Research Centre, Vijayapur.

B.L.D.E. UNIVERSITY'S

SHRI B. M. PATIL MEDICAL COLLEGE, HOSPITAL

& RESEARCH CENTRE, VIJAYAPUR

COPYRIGHT

DECLARATION BY THE CANDIDATE

Date: **Dr.NANDISH H R**

Place: Vijayapur   Post Graduate Student,

                                   Department of Radiodiagnosis,

                                   B.L.D.E.U's Shri B. M. Patil Medical College,

                                   Hospital & Research Centre, VIJAYAPUR.

LIST OF ABBREVIATIONS USED

ADPKD	-	Autosomal Dominant Polycystic Kidney Disease
ARPKD	-	Autosomal Recessive Polycystic Kidney Disease
AML	-	Angiomyolipoma
AO	-	Aorta
CMP	-	Corticomedullary Phase
CT	-	Computed Tomography
EPN	-	Emphysematous Pyelonephritis
HU	-	Hounsfield Units
IVC	-	Inferior Venacava
IVP	-	Intra Venous Pyelogram
IVU	-	Intra Venous Urogram
MDCT	-	Multidetector Computed Tomography
MRI	-	Magnetic Resonance Imaging
MCN	-	Multilocular Cystic Nephroma
NP	-	Nephrographic phase
RCC	-	Renal Cell Carcinoma
ROI	-	Region Of Interest
SPECT	-	Single Photon Emission Computed Tomography
TCC	-	Transitional Cell Carcinoma
US	-	Ultra Sound
WW	-	Window width
WL	-	Window Length

ABSTRACT

PURPOSE

To study the role of triphasic (unenhanced, corticomedullary and nephrographic phases) multidetector computed tomography in the detection and characterization of renal masses and to study the enhancement pattern of renal parenchyma.

MATERIAL AND METHODS

This was a cross sectional prospective study which included 30 consecutive cases of renal masses detected on MDCT. The post biopsy or surgical data were used as a reference standard. The patient's age, gender and tumour size and CT features including septations, calcification, density, margins, wall irregularity were analysed. In addition enhancement pattern and enhancement in corticomedullary and nephrographic phases were analysed. Chi square test was used to assess the association between subtype of renal masses (benign or malignant) and gender, morphological features, and type of contrast enhancement. To assess the association between benign and malignant masses with respect to age, size of lesion, contrast enhancement in corticomedullary and nephrographic phases student T test was used. The diagnostic efficacy and cut off values of enhancement and degree of enhancement in various phases was determined by reciever operating characteristic (ROC) curve. The curves were analysed for cut off values to differentiate RCC from other masses. In all our analysis p value < 0.05 was significant.

RESULTS

The mean age of patients was 53 ± 12 years (range 26 to 82 years) which include 19 males and 11 females. 7 out of 13 (53.8 %) cases of RCC were seen in the age group of 50 to 60 years with a mean age of 60.77 years. The male to female sex

ratio in patients with RCC was 2.2 : 1 which included 9 males and 4 females. The most common presentation of renal masses in our setting was loin pain which was seen in 25 out of 30 cases (83 %).

The renal cortex demonstrated a mean attenuation of 32 ± 3 HU on unenhanced CT images. Cortical mean enhancement was 122 ± 15 HU during corticomeduallary phase and 137 ± 9 HU during nephrographic phase.

Out of 30 cases, 14 cases were benign and 15 were malignant masses. The mean attenuation value of malignant masses in unenhanced CT images was 34.8 HU where as in benign masses was 9.2 HU. In corticomedullary phase the malignant masses showed rapid enhancement with a mean HU value of 96.53 ± 12.977 and a rapid decrease of in enhancement in following nephrographic phase with mean HU value of 72.93 ± 10.194. The ROC curve analysis showed that the cut off values with highest sensitivity and specificity for characterization of RCC from other masses was 71.5 HU in corticomedullary phase (sensitivity 100%, specificity 99.9%), 41.5 HU in nephrographic phase (sensitivity 100% , specificity 99.8 %).

CONCLUSION

For characterization of renal masses the enhancement pattern and enhancement in corticomedullary and nephrographic phases are useful parameters in differentiating benign from malignant masses.

The malignant masses demonstrated greater enhancement in corticomedullary phase than in nephrographic phase.

The normal renal cortex demonstrated greater enhancement in nephrographic phase than in corticomedullary phase.

MDCT protocol for evaluation of renal masses should include unenhanced, corticomedullary and nephrographic phases for better detection and characterization of renal massses.

TABLE OF CONTENTS

Sl. No	Tables	Page No
1.	INTRODUCTION	1
2.	OBJECTIVES OF THE STUDY	3
3.	REVIEW OF LITERATURE	4
4.	METHODOLOGY	51
5.	RESULT	56
6.	DISCUSSION	90
7.	CONCLUSIONS	99
8.	LIMITATION	100
9.	SUMMARY	101
10.	BIBLIOGRAPHY	103
11.	ANNEXURE	113

LIST OF TABLES WITH CORRESPONDING GRAPHS

LIST OF FIGURES

INTRODUCTION

Ultrasonography, CT and MRI are used in the detection and characterization of renal masses.

Ultrasonography is used as a screening modality in the detection of renal masses but it is neither sensitive nor specific in the characterization of lesion as benign or malignant. The capability of US to detect a renal mass depends from technical and anatomical factors that influence the diagnostic performance.

MRI is as sensitive and specific as CT in detection, characterization and staging of solid masses. The well known advantages of MR imaging, as multiplanar imaging, MR angiography and tissue characterization, can be nowadays obtained even with MDCT that has the similar capabilities. but MRI due to its high cost and its long image acquisition time, causes motion artifacts, hence it cannot be used in our setting.

CT is considered to be the state of the art technology in the evaluation of abdomen. It is widely accepted as a preferred imaging technique because of its low cost, high accuracy and ready accessibility.

The most recent technical advances, obtained with the use of multidetector CT (MDCT) and with multiple reconstruction software, allow a significant reduction of the scanning time associated with increased spatial resolution. The reduced gantry rotation times (0.5 s or less) allow about 25 times faster scanning times than traditional single row helical CT. Faster scan times results in decreased breath-hold times with reduction of motion artifacts. The use of thinner slice thickness is associated to better quality volume data set for workstation analysis and multiplanar reformation (MPR): thus, three dimensional (3-D) imaging and volume reconstructions are possible, with more and improved diagnostic images. The main

advantages of MDCT are faster scanning time, increased volume coverage and improved spatial and temporal resolution [1]

Renal cell carcinoma (RCC) is the most common adult renal epithelial cancer, accounting for more than 90% of all renal malignancies [2]. RCC is the most lethal of all urologic cancers. The 5-year cancer-specific survivals of patients with pT4 RCC and lymph node metastases are 20% and 5%–30%, respectively. There is continued global increase in the incidence of RCC, partly due to early diagnosis with cross sectional imaging modalities

Other malignant masses include transitional cell carcinoma (TCC), lymphoma (primary and more frequent secondary), metastases from carcinoma and primary/secondary sarcoma.

Benign tumours account for approximately 20% of all solid renal cortical tumours, and renal oncocytoma is the most common solid tumour type.

Non-neoplastic renal masses include inflammatory pseudotumours with and without abscess formation, renal infarct, haematoma and replacement lipomatosis with coexistent xanthogranulomatous pyelonephritis.

The great majority of renal masses are found incidentally on imaging. most of these - benign. Some are malignant and need to be surgically removed.
Therefore, the proper characterization of these masses is essential so that appropriate management is instituted.

The purpose of our study is to compare thin-section corticomedullary and nephrographic phase images of the kidneys to determine whether one of these phases of parenchymal enhancement is superior in the characterization of a previously detected indeterminate renal mass.

OBJECTIVE OF THE STUDY

- To study attenuation and enhancement pattern of renal masses during unenhanced, corticomedullary and nephrographic phases.

- To evaluate the characteristics of renal parenchymal enhancement during corticomedullary and nephrographic phases.

- To compare computed tomography finding with pathological diagnosis, Where ever possible.

METHODOLOGY

Source of data:

Patients with suspected (hematuria, flank pain , flank fullness) or incidentally /utrasonographically detected renal mass referred for CT scan of abdomen to the Department of Radiodiagnosis, Shri B.M. Patil Medical College Hospital and research center, Bijapur. Patients with renal masses on CT imaging were included in this study.

Sample size: 30 patients were included in the study.

Period of Study: July 2014 - June 2016.

Study Design: Cross sectional study.

Inclusion criteria: All patients with renal mass on CT abdomen were included irrespective of age and sex.

Exclusion criteria:

- Simple renal cyst (Bosniak category 1) – confirmed on ultrasonography.
- Renal trauma.
- Extra renal mass invading renal parenchyma.

Technique for CT

All CT scans were done using Philips brilliance 6 – slice MDCT with 120 KVp and 300 mAs with 5 mm slice thickness. The scan parameters remained constant throughout the study.

Patients were kept nil orally 4 hrs prior to the CT scan to avoid complications while administrating contrast medium. The patients are given 500–750 mL of water to drink over a 15–20 minute period before the start of the examination. Risks of contrast administration were explained to the patient and consent was obtained prior to the contrast study. Routine anterio-posterior topogram of the abdomen was initially

taken in all patients in the supine position with the breath held. Axial plain sections of 5 mm thickness was taken from the level of lung bases to the level ischial tuberosities. The imaging protocols for renal CT were: precontrast or noncontrast scan, corticomedullary phase, and nephrographic phase.

In all cases plain scan was followed by intravenous contrast scan in suspended inspiration.

The noncontrast scans are always necessary to obtain a baseline for measurements of enhancement after contrast agent administration and to detect intratumoral or marginal calcifications that can be very small and faint.
100–120 mL of Iohexol (Optiscan 350)contrast medium was injected to antecubital vein at a rate of 3 mL/sec.

The corticomedullary (angionephrographic) phase starts at about 30–40 seconds after the start of contrast medium injection. There is intense enhancement of the renal cortex due to preferential arterial flow to the cortex and glomerular filtration of the contrast material, while the medulla remains relatively less enhanced. This is also the best phase for maximum opacification of the renal veins.

The nephrographic phase begins at 80–120 seconds after the start of contrast medium injection. Tubular filtration of contrast material produces homogeneous enhancement of the renal parenchyma. This is the best phase for detection of subtle parenchymal lesions.

Post study reconstructions were done at 2.5 mm. Sagittal and coronal reconstructions were made wherever necessary. Newer techniques in Multislice CT like curved planar reformatting, volume rendering, Maximum and Minimum Intensity Projections were done as and when necessary. The magnification mode was commonly employed, and the scans were reviewed on a direct display console at

multiple window settings (i.e. abdomen window at 320/40; Lung window 1400/-600; Bone window of 2400/200)

The pathological lesions were evaluated with respect to pre and post contrast attenuation values, the size, location of the mass, presence of calcification , presence of fat, and extension into the adjoining structures. Image analysis: All CT diagnosis were obtained by a consensus of two senior radiologists. The size and location of the mass in question were obtained from the nephrographic images. The mass was then characterized by evaluating its features and by presence or absence of contrast enhancement. The attenuation values were measured in unenhanced, corticomedullary and nephrographic phase images by the region-of-interest technique.

The enhancement of all lesions was determined for both corticomedullary and nephrographic phases by measuring the difference in attenuation numbers between the contrast enhance and unenhanced images.

Renal cortical enhancement was also determined for both corticomedullary and nephrographic phases by measuring the difference in cortical attenuation numbers between the contrast enhanced and unenhanced images.

Enhancement parameters that were calculated include renal mass enhancement and renal cortical enhancement during corticomedullary and nephrographic phases. These were analyzed and compared for each patient and the summary enhancement data were tested for statistical significance by using the Student test.

All solid lesions with attenuation similar to other soft tissue abdominal structures and if interrogation of region of interest revealed tissue enhancement of 10 HU or greater were classified as malignant.

For characterization of cystic renal lesions, the Bosniak criteria were used. [3]

Bosniak I: Benign simple cyst, hairline-thin wall, no septa, calcifications or solid components. Water density, no contrast enhancement.

Bosniak II: Benign cyst, may contain few hairline-thin septa. Fine calcification or slightly thickened calcification in wall or septa. Uniformly high-attenuation lesions (<3 cm), sharply marginated, no enhancement, are included in this group.

Bosniak IIF: Increased number of hairline-thin septa. Minimal enhancement in hairline-thin smooth septum or wall, minimal thickening of the septa or wall. Possibly thick and nodular calcification, no contrast enhancement. No enhancing soft-tissue components. Totally intrarenal nonenhancing high-attenuation renal lesions that are 3 cm or larger are also included in this category. These lesions are generally well marginated. &

Bosniak III: Indeterminate cystic masses with thickened irregular walls or septa, enhancement can be seen.

Bosniak IV: Clearly malignant cystic masses, additionally with enhancing soft-tissue components adjacent to but independent of the wall or septa.

Brief history of Computed tomography [(4)]

Computed Tomography (CT) imaging is also known as "CAT scanning" (Computed Axial Tomography). Tomography is from the Greek word *"tomos"* meaning "slice" or "section" and *"graphia"* meaning "describing".[(4)]

CT was invented in 1972 by British engineer Godfrey Hounsfield of EMI Laboratories, England and by South Africa-born physicist Allan Cormack of Tufts University, Massachusetts. Hounsfield and Cormack were later awarded the Nobel Peace Prize for their contributions to medicine and science.

The first clinical CT scanners were installed between 1974 and 1976. The original systems were dedicated to head imaging only, but "whole body" systems with larger patient openings became available in 1976. CT became widely available by about 1980.

The basic components of a standard diagnostic CT scanner include an X-ray source and a detector, positioned on opposite ends of the patient, mounted on a rotational gantry that can spin this imaging chain at very high speeds. A cross-sectional image is created by mathematical reconstruction of the measured X-ray intensities received by the detector at different positions around the patient in a circular orbit.

The first CT scanner developed by Hounsfield in his lab at EMI took several hours to acquire the raw data for a single scan or "slice" and took days to reconstruct a single image from this raw data. The latest multi-slice CT systems can collect up to 4 slices of data in about 350 ms and reconstruct a 512 x 512-matrix image from millions of data points in less than a second.

CT has made great improvements in speed, patient comfort, and resolution. As CT scan times have gotten faster, more anatomy can be scanned in less time. Faster

scanning helps to eliminate artifacts from patient motion such as breathing or peristalsis. CT exams are now quicker and more patient-friendly than ever before. Tremendous research and development has been made to provide excellent image quality for diagnostic confidence at the lowest possible x-ray dose.

MDCT (MULTI DETECTOR ROW COMPUTED TOMOGRAPHY)

The first scanner with more than one row of detectors and a widened z-axis x-ray beam was introduced by Elscint in 1992 (CT-Twin). The ''modern MDCT '' were introduced in late 1998.

The primary difference between single-slice CT (SSCT)and MDCT hardware is in the design of the detector arrays. SSCT detector arrays are one dimensional; that is, they consist of a large number (typically 750 or more) of detector elements in a single row across the irradiated slice to intercept the x-ray fan beam. In the slice thickness direction (z-direction), the detectors are monolithic, that is, single elements long enough (typically about 20 mm) to intercept the entire x-ray beam width, including part of the penumbra (here, the term ''x-ray beam width'' always refers to the size of the x-ray beam along the z-axis—that is, in the slice thickness direction). In MDCT, each of the individual, monolithic SSCT detector elements in the z-direction is divided into several smaller detector elements, forming a 2-dimensional array. Rather than a single row of detectors encompassing the fan beam, there are now multiple, parallel rows of detectors. [1]

In MDCT, the slice thickness is determined by detector configuration and not x-ray beam collimation.

HELICAL MDCT

Helical ("spiral") CT image acquisition was a major advance on the earlier stepwise ("stop and shoot") method.

Helical scanning with MDCT scanners is conceptually identical to that with single slice CT scanners.

With helical CT, the patient is moved through a rotating x-ray beam and detector set. From the perspective of the patient, the x-ray beam from the CT traces a helical path. The helical path results in a three-dimensional data set, which can then be reconstructed into sequential images for a stack.

Advantages of MDCT

The introduction of MDCT was a milestone with regard to increased scan speed, improved z-axis spatial resolution, and better utilization of the available x-ray power. For the first time, volume data could be acquired without misregistration of anatomic detail. Volume data became the basis for applications such as CT angiography, which has revolutionized the noninvasive assessment of vascular disease. The ability to acquire volume data also paved the way for the development of three-dimensional (3D) image processing techniques such as multiplanar reformation (MPR), maximum intensity projection, surface-shaded display, and volume-rendering techniques, which have become a vital component of medical imaging today. [1]

DEVELOPMENT OF KIDNEY SYSTEMS

Three slightly overlapping kidney systems are formed in a cranial to caudal sequence during intrauterine life in humans: the pronephros, mesonephros, and metanephros. The first of these systems is rudimentary and nonfunctional; the second may function for a short time during the early fetal period; the third forms the permanent kidney.

PRONEPHROS

At the beginning of the fourth week, the pronephrosis represented by 7 to 10 solid cell groups in the cervical region. These groups form vestigial excretory units,

nephrotomes, that regress before more caudal ones are formed. By the end of the fourth week, all indications of the pronephric system have disappeared.

MESONEPHROS

The mesonephros and mesonephric ducts are derived from intermediate mesoderm from upper thoracic to upper lumbar (L3) segments . Early in the fourth week of development, during regression of the pronephric system, the first excretory tubules of the mesonephros appear. They lengthen rapidly, form an S-shaped loop, and acquire a tuft of capillaries that will form a glomerulus at their medial extremity. Around the glomerulus the tubules form Bowman's capsule, and together these structures constitute a renal corpuscle. Laterally the tubule enters the longitudinal collecting duct known as the mesonephric or wolffian duct .In the middle of the second month the mesonephros forms a large ovoid organ on each side of the midline

Since the developing gonad is on its medial side, the ridge formed by both organs is known as the urogenital ridge. While caudal tubules are still differentiating, cranial tubules and glomeruli show degenerative changes, and by the end of the second month the majority have disappeared. In the male a few of the caudal tubules and the mesonephric duct persist and participate in formation of the genital system, but they disappear in the female.

METANEPHROS:

The Definitive Kidney

The third urinary organ, the metanephros, or permanent kidney, appears in the fifth week. Its excretory units develop from metanephric mesoderm in the same manner as in the mesonephric system. The development of the duct system differs from that ofthe other kidney systems.

Collecting System - Collecting ducts of the permanent kidney develop from the ureteric bud, an outgrowth of the mesonephric duct close to its entrance to the cloaca . The bud penetrates the metanephric tissue, which is molded over its distal end as a cap. Subsequently the bud dilates, forming the primitive renal pelvis, and splits into cranial and caudal portions, the future major calyces.

Each calyx forms two new buds while penetrating the metanephric tissue. These buds continue to subdivide until12 or more generations of tubules have formed Meanwhile, at the periphery more tubules form until the end of the fifth month. The tubules ofthe second order enlarge and absorbthose of the third and fourth generations, forming the minor calyces of the renal pelvis.

During further development, collecting tubules of the fifth and successive generations elongate considerably and converge onthe minor calyx, forming the renal pyramid . The ureteric bud gives rise to the ureter, the renal pelvis, the major and minor calyces, and approximately 1 million to 3 million collecting tubules.

NORMAL ANATOMY

The kidneys:

The kidneys lie in the superior part of the retroperitoneum on either side of the vertebral column at approximately the levels of L1–L4. The right kidney usually lies slightly lower than the left, due to the bulk of the liver. The kidneys move up and down by 1–2 cm during deep inspiration and expiration. In the adult, the bipolar length of the kidney is usually approximately 11 cm. Discrepancy between right and left renal length of up to 1.5 cm is within normal limits. The upper poles of the kidneys lie more medial and posterior than the lower poles. The kidneys are surrounded by a layer of fat, the perinephric fat, which is encapsulated by the perinephric fascia (Gerota's fascia)

The kidney is covered by a fibrous capsule, which is closely applied to the renal cortex. The renal cortex forms the outer third of the kidney. Columns of cortex (columns of Bertin) extend medially into the medulla between the pyramids. The renal medulla lies deep to the cortex and forms the inner two thirds. The medulla contains the renal pyramids, which are cone-shaped, with the apex (the papilla) pointing into the renal hilum. The medullary rays run from the cortex into the papilla. Each papilla projects into the cup of a renal calyx, which drains via an infundibulum into the renal pelvis . The renal pelvis is a funnel-shaped structure at the upper end of the ureter. It normally divides into two or three major calyces: the upper and lower pole calyces and in some cases a third calyx between those at each pole. Each major calyx then divides into two or three minor calyces, which have a cup-shape, indented by the apex of the accompanying renal pyramid. The renal hilum contains the renal pelvis, the renal artery, the renal vein and lymphatics, all of which are surrounded by renal sinus fat.

Renal arteries, veins and lymphatic drainage:

The right and left renal arteries arise from the abdominal aorta, at approximately the level of the superior margin of L2, immediately caudal to the origin of the superior mesenteric artery . There is usually a single artery supplying each kidney, although there are many anatomical variants, with up to four renal arteries supplying each kidney. The renal artery divides in the renal hilum into three branches. Two branches run anteriorly, supplying the anterior upper pole and entire lower pole, and one unsposteriorly supplying the posterior upper pole and mid pole.

Five or six veins arise within the kidney and join to form the renal vein, which runs anterior to the artery within the renal pelvis. The right renal vein has a short course, running directly into the IVC. The left renal vein runs anterior to the

abdominal aorta and then drains into the IVC. Occasionally, the left renal vein runs posterior to the aorta, known as a retro-aortic renal vein. The left renal vein receives tributaries from the left inferior phrenic vein, the left gonadal and the left adrenal vein.

The lymphatic drainage of the kidneys follows the renal arteries to nodes situated at the origin of the renal arteries in the para-aortic region.

Nerve supply:

The sympathetic nerves supplying the kidney arise in the renal sympathetic plexus and run along the renal vessels. Afferent fibres, including pain fibers, travel with the sympathetic fibers through the splanchnic nerves and join the dorsal roots of the 11th and 12th thoracic and the 1st and 2nd lumbar levels.

Fascial spaces around the kidney:

The kidney is surrounded by perirenal fat, which is completely encircled by a fascial plane (Gerota's fascia), which also encases the suprarenal gland . Medially, Gerota's fascia blends with the fascia surrounding the aorta and IVC.

COMPUTED TOMOGRAPHY OF KIDNEYS

Multiplanar imaging of the kidneys can provide exquisite anatomic detail. The densities of the renal medulla and renal cortex on non-enhanced CT are very similar, and they are similar to the attenuation of the liver. The renal parenchyma typically ranges from 27 to 47 Hounsfield units on non-enhanced CT. [5]

The renal sinus is most commonly anterior and medial to the parenchymal tissue, and it is easily differentiated from the parenchyma by its fat attenuation, even without intravenous contrast. The central renal sinus has fat attenuation with linear fluid-attenuation renal vessels coursing from the aorta and toward the inferior vena

cava. The urothelial tract also originates in the renal sinus fat at the anteromedial aspect of the kidney, and in this region it includes the renal calyces and renal pelvis.

The appearance of the kidneys varies with the timing of delay until image acquisition after the injection of intravenous iodinated contrast. On nonenhanced CT, the central medullary portion of the parenchyma is not differentiated from the cortex in normal kidneys. Within 15 to 25 seconds of injection of intravenous contrast, the aorta and renal arteries opacify with contrast, as may be seen in CT angiography.

During arterial phase of contrast enhancement, the cortex and medulla enhance at different rates with bright cortex juxtaposed to the less enhanced medulla. With standard injection rates, the cortex enhances to 70 HU during arterial phase and doubles to 145 HU within 40 seconds after injection. The medulla only enhances to less than 60 HU by 50 seconds. At approximately 100 to 120 seconds after contrast injection, during the nephrographic phase, the enhancement of the cortex and medulla equilibrates measuring at least 120 HU. The renal parenchyma of a normal kidney is homogeneous in the nephrographic phase with sharp delineation of the non-enhancing central renal sinus fat.

After atleast 3 minutes after injection, excretion from the renal tubules begins to fill the renal calyces and renal pelvis, known as the excretory phase. At this time, the renal medulla may be slightly more enhanced than the cortex as contrast is excreted from the renal tubules. During the excretory phase, dense contrast fills the collecting systems, the ureters, and eventually the urinary bladder.(6)

Birnbaum et al [5] prospective study of 30 patients was undertaken with CT to characterize "indeterminate" renal masses. The mean attenuation of renal cortex was 19 HU ± 5 (range,7-25 HU) on unenhanced CT images. When the corticomedullary phase was performed at 30–33 seconds Cortical enhancement averaged 53 HU ± 34

and the nephrographic phase was performed at 120 seconds, the renal cortex progressively increased in enhancement. The renal cortex demonstrated a mean attenuation 116 HU ± 29 (range, 61-181 HU) for nephrographic-phase images.

Cohan et al. [7] studied cortical enhancement in corticomedullary and nephrographic phases in 33 cases. Mean attenuation of renal cortex in their study was 147 ± 41 HU on corticomedullary phase images and 117±41 HU on nephrographic phases images. They found that mean attenuation was 30 HU greater in corticomedullary phase than in nephrographic phaseimages.

Szolar et al. [8] studied 93 cases, mean cortical attenuation was 185 ±35 HU in corticomedullary phase and 168 ±33HU in nephrographic phase. In their study, although mean cortical enhancement was slightly greater in corticomedullary phase images than that in nephrographic phase images, this was not statistically significant.

NORMAL ENHANCEMENT OF RENAL PARENCHYMA
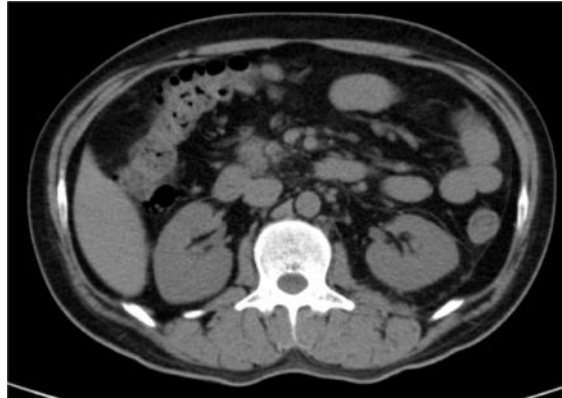
UNENHANCED CT IMAGE

CORTICOMEDULLARY PHASE
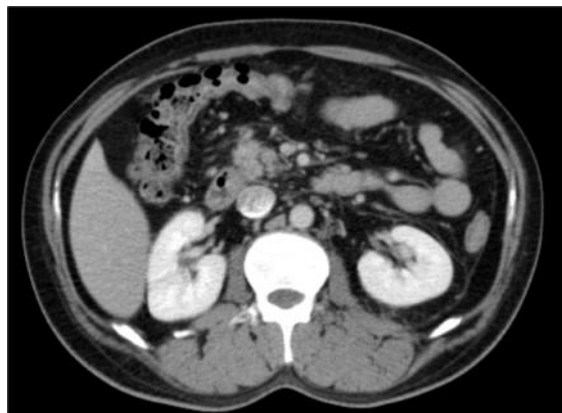
NEPHROGRAPHIC PHASE

RADIOGRAPHIC EVALUATION OF RENAL MASSES

Several modalities are currently available for detecting and evaluating renal masses. A systematic method is necessary to ensure complete evaluation of suspected renal masses because each radiographic modality has its relative strengths and weaknesses.

Intravenous pyelography (IVP), despite its lack of sensitivity and specificity, remains the initial diagnostic method in many cases because of its role in evaluation of hematuria. Hematuria is the most common presenting complaint in patients with renal cell carcinoma (occurring in 50%-66% of patients), only approximately 3%-6% of patients with hematuria will prove to have renal cell neoplasms. [9]

Intravenous pyelography with or without nephrotomography can detect many renal masses and provide information regarding the function of the kidneys. The acceptance of Intravenous pyelography as an adequate screen for renal masses has rested on the twin assumptions that small renal tumors are benign and that Excretory Urography enables detection of all malignant renal tumors. With the advent of cross-sectional imaging techniques, both assumptions have been questioned. **Kass et al.** [10] described four patients with malignant renal masses and a normal Intravenous pyelography study. The largest mass in this series was 4 X 4 X 3 cm. An IVP may miss small anterior or posterior lesions that do not distort the collecting system or the periphery of the kidney. [11]

David M. Warshauer et al. [12] conducted a study to determine the relative sensitivities and specificities of Excretory Urography/ Linear Tomography, US, and CT for the diagnosis of renal parenchymal masses. A prospective blinded study of 201 patients was performed. CT disclosed 204 renal parenchymal masses. Ninety-six percent of the lesions were shown by US or CT to be simple cysts. All cases of RCC

were detected by Excretory Urography, CT, and US. Two of the four lesions seen in the case of von Hippel-Lindau disease and three of the four metastatic lesions in another case were missed at Excretory Urography and detected only at CT. Overall, Excretory Urography permitted identification of 10% of CT-detected masses less than 1 cm in size, 21% of lesions greater than or equal to 1 but less than 2 cm, 52% of lesions greater than or equal to 2 cm but less than 3 cm, and 85% of lesions 3 cm or more. In the 133 patients in whom US was also performed, US permitted identification of 26% of CT-detected masses less than 1 cm, 60% of lesions greater than or equal to 1 but less than 2 cm, 82% of lesions greater than or equal to 2 but less than 3 cm, and 85% of lesions 3 cm or greater. Excretory Urography has fairly good sensitivity for lesions greater than 3 cm in diameter. For lesions less than 3 cm, sensitivity fell off sharply. US and Excretory Urography had similar sensitivities for masses 3 cm or more in diameter. For lesions less than 3 cm but greater than or equal to 2 cm, US, unlike Excretory Urography, maintained sensitivity above 80%. CT may have a role not only in evaluation of cases in which excretory urographic results are questionable on positive but also in confirmation of apparently negative excretory urographic or US findings when clinical suspicion of a lesion is high.

When a renal mass is identified by IVP, ultrasonography/ CT should be the next study performed.

Ultrasonography reliable in differentiating solid tissue from fluid and can establish the diagnosis a simple cyst. Strict sonographic criteria for simple cysts have been defined and include a smooth cyst wall, a round or oval shape without internal echoes, and thorough transmission with strong acoustic shadows posterio rly. If these criteria are met, observation is sufficient in an asymptomatic patient.[3]

Sonography is generally the first choice because it costs less than CT, and no ionizing radiation or contrast material is required.

Sonography is the most cost-effective imaging method for the workup of a renal mass detected at urography. The number of sonographic examinations In which findings are indeterminate or positive (for a solid mass) is not sufficiently high to warrant replacement of sonography by CT, regardless of the size and location of the lesion.[13]

A substantial number of lesions cannot be definitively charactenized, because of such factors as the patient's habitus or the location of the lesion in the left upper pole of the kidney.[14]

The advent of multi detector CT scan has enabled us to delineate the mass, detect and map the extent of venous spread, lymph nodal enlargement and diagnose local or distant spread.[15]

In general, any renal mass that enhances with intravenous contrast on CT scanning should be considered a renal cell carcinoma until proved otherwise.

Although MRI can detect and characterize many large renal masses, the spatial resolution is insufficient for diagnosis of small intraparenchymal lesions.

WHO histological classification of tumours of the kidney [2]

Renal cell tumours

Renal cell carcinoma

Carcinoma associated with neuroblastoma

Mucinous tubular and spindle cell carcinoma

Papillary adenoma

Oncocytoma

Metanephric tumours

Nephroblastic tumours

Mesenchymal tumours Sarcomas, Haemangiopericytoma, Angiomyolipoma , Epithelioid angiomyolipoma, Leiomyoma, Haemangioma , Lymphangioma

Mixed mesenchymal and epithelial tumours

Neuroendocrine tumours

Haematopoietic and lymphoid tumours - Lymphoma

Germ cell tumours

Metastatic tumours

WHO histological classification of Tumours of the renal pelvis and ureter

Epithelial

Malignant epithelial tumours - Urothelial neoplasms, Squamous cell carcinoma, Adenocarcinoma

Benign epithelial tumours – papilloma, adenoma

Non-epithelial tumours of renal pelvis and ureter

Malignant tumours - sarcomas

Benign tumours - Fibroepithelial polyps leiomyoma, haemangioma, and periureteric lipoma

Miscellaneous tumours - Neuroendocrine tumours , Lymphoma

Renal Pseudotumors [16]

Prominent Columns of Bertin

Dromedary Hump

Persistent Fetal Lobulation (Lobation)

Infectious Renal Pseudotumors - Focal Pyelonephritis, Renal Abscess, Scarred Kidney

Granulomatous Renal Pseudotumors - Xanthogranulomatous Pyelonephritis (XGP), Other Granulomatous Renal Pseudotumors

Vascular Renal Pseudotumors - Arteriovenous Malformation (AVM), Subepithelial Renal Pelvic Hematoma, Extramedullary Hematopoiesis.

CYSTIC LESIONS OF KIDNEY

The most common renal mass in the adult is a cyst. Simple renal cysts arise from the cortex. The criteria for the diagnosis of cyst using CT are (a) sharp margination and demarcation from surrounding renal parenchyma; (b) smooth, thin wall; (c) water density content which ishomogeneous throughout (0-20 HU); and (d) no enhancement following Intravenous administration of contrast material.[3]

Depending on the size, attenuation values, thickness of the septa and presence of mural components, Bosniak has classified renal cysts into following category to assess the risk of malignancy and further management. [3]

Category I - A benign simple cyst with a hairline-thin wall that does not contain septa, calcifications, or solid components; it has water attenuation and does not enhance; no intervention is needed

Category II A benign cystic lesion that may contain a few hairline-thin septa in which perceived (not measurable) enhancement may be appreciated; fine calcification or a short segment of slightly thickened calcification may be present in the wall or septa; uniformly high-attenuating lesions (3 cm) that are sharply marginated and do not enhance are included in this group; no intervention is needed

Category IIF Cysts may contain multiple hairline-thin septa; perceived (not measurable) enhancement of a hairline-thin smooth septum or wall can be identified;

there may be minimal thickening of wall or septa, which may contain calcification that may be thick and nodular, but no measurable contrast enhancement is present; there are no enhancing soft-tissue components; totally intrarenal nonenhancing high-attenuating renal lesions (3 cm) are also included in this category; these lesions are generally well marginated; they are thought to be benign but need follow-up to prove their benignity by showing stability

Category III Cystic masses with thickened irregular or smooth walls or septa and in which measurable enhancement is present; these masses need surgical intervention in most cases, as neoplasm cannot be excluded; this category includes complicated hemorrhagic or infected cysts, multilocular cystic nephroma, and cystic neoplasms; these lesions need histologic diagnosis, as even gross observation by the urologist at surgery or the pathologist at gross pathologic evaluation is frequently indeterminate

Category IV Clearly malignant cystic masses that can have all of the criteria of category III but also contain distinct enhancing soft-tissue components independent of the wall or septa; these masses are clearly malignant and need to be removed

Cysts are usually asymptomatic. However, they may cause hematuria, and, if large, they may cause compressive mass effect, which can lead to hypertension or obstruction of the collecting system. Cysts may be solitary or multiple, and they can arise anywhere in the kidney. They tend to increase in size and number with age.

A simple cyst may become complicated as a result of hemorrhage, infection, or other processes that thicken some or the entire wall and may increase the attenuation of the contents.[17,18]

In a study by **Bae KT et al. (2000)** [19], the mean attenuation change in cysts between nonenhanced and contrast-enhanced images was 11.8 HU (SD, 3.8) for the

cortical phase and 13.6 HU (SD, 5.6) for the nephrographic phase images. These values are similar to those obtained in a previous clinical study by **Birnbaum et al** [5]. The larger increase in attenuation in the nephrographic phase was statistically significant and is likely related to the fact that the overall enhancement of the renal parenchyma is greater during the nephrographic phase than the cortical phase. The pseudoenhancement phenomenon was more apparent in small renal cysts (0.6– 1.0 cm) than in large cysts (.1.0 cm). Thus postcontrast enhancement less than 10 HU in a renal mass larger than 1.0 cm can be considered as evidence that the mass is a cyst.

Hyperdense cysts have an attenuation value greater than renal parenchyma on precontrast CT images, commonly measuring 40 to 90 HU. This may be a result of bleeding into the cyst, with concentration of the protein components of blood. Most hyperdense cysts are solitary, but they may be multiple; they are quite common in autosomal dominant polycystic disease. [20–22]

If the lesion is small (most are less than 3 cm), homogeneous, and shows no enhancement on postcontrast images, and if it has no other complicating factor (such as calcification), diagnosis of benign hyperdense cyst can be made. If CT first detects a hyperdense lesion, sonography may be helpful, because it may confirm the cystic nature. Follow-up of hyperdense cysts (with the exception of those in polycystic disease) is prudent to confirm their benign nature, because, rarely, renal carcinoma may have the appearance of a hyperdense cyst. [23,24]

CALYCEAL DIVERTICULA

Calyceeal diverticulum refers to urine containing cystic cavity within the renal parenchyma. The diverticulum is lined by transitional epithelium and surrounded by muscularis mucosae, communicating with the collecting system via a narrow isthmus or infundibulum.

Calyceal diverticula may be discovered on CT as incidental findings or they are imaged for further characterization after sonography, because these lesions may appear complicated, with calculi, debris, or milk of calcium within the diverticulum. (25)

These cystic spaces are lined by transitional epithelium and communicate with the collecting system through a narrow opening.

Gayer et al.[26] described their experience with CT in seven patients with calyceal diverticula; they performed CT with either 5 or 10 mm collimation at 5–10 mm intervals through the renal parenchyma. Unenhanced, post-contrast and delayed phase imaging (15–60 min post-injection) was performed in all patients. Non-contrast scans demonstrated heterogeneous round lesions in all cases measuring up to 2 cm in diameter. The lesions contained high attenuation material of calcific density lying inferiorly within the cystic structure and fluid of water density. Following administration of intravenous contrast, the attenuation of fluid in the upper part of the cyst increased by approximately 20 Hounsfield units. Delayed imaging demonstrated opacification of the entire lesion with a similar density to that of the collecting system, confirming the presence of a calyceal diverticulum

PARAPELVIC CYST

Most cysts seen in the renal hilar region are believed to be of lymphatic origin and are usually called parapelviccysts because of their location. These may be solitary but frequently are multiple. Parapelvic cysts are not true renal cysts but may be lymphatic in origin or develop from embryologic rests. Unlike perinephric cysts which may be the result of urine extravasation, parapelvic cysts do not communicate with the collecting system and, therefore, do not fill with contrast material during excretory urography or contrastenhanced CT.[27]

Hector Hidalgo [28] conducted a retrospective study in which he reviewed 16 patients who had a final diagnosis of a single or multiple parapelvic cysts. A mass within the renal sinus was considered a parapelvic cyst by CT if it had a homogeneous appearance, an attenuation coefficient near water with no enhancement after intravenous infusion of contrast material, and no discernable wall on the part projecting outside the renal margin. Of the 14 cases evaluated by CT, all showed a homogenous cystic mass in the renal pelvis causing distortion of the renal collecting system. Six cases revealed a single unilateral large cyst with a smooth outline with or without any associated hydronephrosis. The other eight cases revealed multiple bilateral cystic masses indenting the collecting system. In these cases the wall between the small cysts could not be identified at some levels giving the appearance of a single lobulated mass. At other levels, however, the individual cysts were separated by the renal collecting system and renal hilar vessels.

Parapelvic cysts are usually asymptomatic and require no therapy, but may lead to hypertension, hematuria,or hydronephrosisor may become secondarily infected. [29]

BENIGN RENAL LESIONS

ONCOCYTOMA

Renal oncocytoma is a benign renal tumour, accounting for approximately 3–7 % of all renal tumours. The peak age of incidence is in the seventh decade. Oncocytoma is hypothesized to originate from or differentiate towards type A intercalated cells of the cortical collecting duct. [30]

Typical imaging findings of renal oncocytoma are described as a homogeneous hypervascular mass with subsequent washout in the delayed phase. A central scar is a characteristic finding, specially in a large oncocytoma [31]

Kim Ji [32] conducted a study to determine the usefulness of segmental enhancement inversion during the corticomedullary phase (CMP) and early excretory phase (EEP) of biphasic multidetector computed tomography (CT) in differentiating small renal oncocytoma from renal cell carcinoma (RCC). Segmental enhancement inversion was defined as follows: In a mass with two segments showing different degrees of enhancement during CMP, the relatively highly enhanced segment became less enhanced during EEP, whereas the less-enhanced segment during CMP became highly enhanced during EEP. 98 patients with pathologically confirmed renal masses smaller than 4 cm (10 renal oncocytomas and 88 RCCs) were included in this study. Eight of 10 renal oncocytomas and only one of 88 RCCs showed segmental inversion during CMP and EEP, which significantly differentiated small renal oncocytomas and RCCs ($P < .0001$). For differentiating oncocytoma from RCC, segmental inversion was found to have a sensitivity of 80% (eight of 10), a specificity of 99% (87 of 88), a positive predictive value of 89% (eight of nine), and a negative predictive value of 98% (87 of 89). The mean values of the attenuation differences shown by two segments during CMP and EEP were 62.75 HU +/- 36.96 (standard deviation) and -36.88 HU +/- 20.02, respectively

Schieda N [33] systematic review to evaluate diagnostic accuracy of segmental enhancement inversion (SEI) at contrast enhanced biphasic multi-detector computed tomography (MDCT) for the diagnosis of renal oncocytoma. Two studies from the same group of investigators demonstrated reasonable diagnostic accuracy (sensitivity 59-80 % and specificity 87 99 %), while two others did not (sensitivity 0-6 %, specificity 93-100 %). Possible reasons for this include timing of biphasic MDCT and methods of interpretation but not size of lesion.

Gakis et al.[34] **and Bird et al.** [35] described that oncocytomas demonstrated greater enhancement than clear cell RCC in the corticomedullary phase. On the other hand, **Young et al.** [36] described that clear cell RCC demonstrated greater enhancement than oncocytoma. **Pierorazio et al.**[37] described that peak enhancement of clear cell RCC was seen predominantly in the corticomedullary phase, while that of oncocytoma was seen predominantly in the nephrographic phase

Zhang et al. [38] described that oncocytoma commonly showed avid enhancement in the venous phase.

ANGIOMYLIPOMA

Angiomyolipoma of the kidney is a neoplasm composed of variable amounts of mature adipose tissue, smooth muscle, and thick-walled blood vessels derived from perivascular epithelioid cells.[39]

Angiomylipoma are commonly sporadic tumors or asocciated with tuberous sclerosis.

Sporadic AML's without tuberous sclerosis are detected in females during the fifth to seventh decade or later and are more often larger and solitary than those found associated with syndromes. Angiomyolipomas may be rarely associated with neurofibromatosis-1, von Hippel-Lindau, or ADPKD.

Angiomylipoma and tuberous sclerosis

Keith A. Casper [40] conducted a study to evaluate renal masses in patients with tuberous sclerosis complex. 59 patients with TSC (mean age, 11.4 years; age range, 3 days to 36 years) were evaluated. There were 31 male and 28 female patients. Angiomyolipomas were identified in 47 (80%) patients and were too numerous to count in 36 (76%), focal in 38 (81%), and bilateral in 42 (89%). The mean largest

diameter was 21 mm. The mean age at which angiomyolipoma was detected in this group was 9.2 years.

The angiomyolipomas were characterized as focal well-defined masses in 38 patients and diffuse infiltrative masses in three. Six patients had both well-defined and infiltrative masses. Of the patients who underwent CT, one demonstrated intralesional hemorrhage, one demonstrated extrarenal hemorrhage, and one demonstrated an intralesional aneurysm. In follow-up examinations, size and/or number increased in 32 (40%) angiomyolipomas. The study concluded that Angiomyolipomas were more common than cysts and tend to be numerous in tuberous sclerosis.

Renal AMLs consist of two distinct histologic subtypes, classic triphasic and monotypic epithelioid. Epithelioid AMLs typically do not show macroscopic fat and appear as soft-tissue masses and are thus indistinguishable from other solid renal masses. This rare subtype of AML is potentially malignant and may exhibit aggressive biology, including recurrence, metastasis, and death.

Kim et al. (2004) [41] : conductred a study to compare various computed tomographic (CT) features of angiomyolipoma (AML) with minimal fat with those of size-matched renal cell carcinoma (RCC). Eighty-one patients (19 with AML with minimal fat [mean diameter, 2.8 cm; range, 1.5–4.5 cm] and 62 with RCC [mean diameter, 3.1 cm; range, 1.8–4.5 cm]) who had undergone biphasic CT (ie, CT with unenhanced, corticomedullary, and early excretory phase scanning) were evaluated. Homogeneous enhancement (observed in 79% of AMLs vs 5% of RCCs; odds ratio, 37) and prolonged enhancement pattern (observed in 58% of AMLs vs 10% of RCCs; odds ratio, 42) were valuable predictors for differentiating AML with minimal fat from RCC at multivariate analysis (P .05 for both). When both CT findings were used as a criterion for differentiating AML from RCC, positive and negative predictive

values were 91% (10 of 11 tumors) and 87% (61 of 70 tumors), respectively. Fifty-three percent of AMLs versus 13% of RCCs showed high tumor attenuation on unenhanced scans (P .04), whereas RCCs showed greater mean enhancement than AMLs (114 HU 44 [SD] vs 73 HU 30 in corticomedullary phase and 66 HU 24 vs 49 HU 20 in early excretory phase) and a male predominance (male-to-female ratio, 50:12 vs 8:11; P .001). They concluded that the gradual enhancement pattern was a useful predictor of AML without visible fat against RCC.

Davenport MS et al. (2011) [42] in his study to determine the optimal Hounsfield unit threshold and region of interest (ROI) size required to accurately diagnose renal angiomyolipoma (AML) and differentiate it from renal cell carcinoma (RCC). The study included 217 RCCs and 65 AMLs. With an attenuation threshold of -10 HU or lower at nonenhanced CT, RCC would be misdiagnosed as AML in 11 (5.1%) cases, one (0.5%) case, and one (0.5%) case with use of the tiny, small, and medium ROIs, respectively. With use of the tiny, small, and medium ROIs, misdiagnosis rates would be 2.3%, 0.5%, and 0.5%, respectively, at a threshold of -15 HU or lower and 1.8%, 0%, and 0%, respectively at a threshold of 20 HU or lower.

In conclusion Nonenhanced CT images were superior to nephrographic phase CT images for the diagnosis of AML. An attenuation threshold of -10 HU or lower with an ROI of at least 19–24 mm is optimal for the diagnosis of AML.

Koichiro Yamakado [43] contucted a study to evaluate the Relationships between Tumor Size, Aneurysm Formation, and Rupturein Renal Angiomyolipoma Twenty-three patients with renal angiomyolipoma were examined with angiography and computed tomography (CT). Sixteen patients had a solitary lesion in one kidney. Six patients had multiple (more than five) tumors in both kidneys, and one patient had multiple tumors in one kidney. Intratumoral hemorrhage and subcapsular and

perirenal hematoma suggestive of rupture were observed in seven patients who had a total of eight tumors. Therefore eight angiomyolipomas were hemorrhagic; the remaining 21 were not hemorrhagic.

There was a significant difference in tumor size between the ruptured (11.4 cm 5.5; range, 4.8–18.0 cm) and the unruptured (5.0 cm +/- 3.1; range, 1.5–11 cm). All ruptured angiomyolipomas wer When tumor sizes of 4 cm or larger and 6 cm or larger were used as predictors of rupture, sensitivity and specificity, respectively, were 100% and 38% for the former criterion and 100% and 67% for the latter criterion e larger than 4 cm (100%, eight of eight)

Aneurysm formation was observed in 22 (76%) of all 29 tumors. There was a tendency that aneurysms were found at a higher rate in the group with ruptured angiomyolipoma than in the group with unruptured angiomyolipoma (100% vs 67%, P .15). Mean aneurysm size was significantly larger in the group with ruptured tumor (13.3 mm 6.2; range, 5–22 mm) than in the group with unruptured tumor (2.4 mm 2.9; range, 2–11 mm; P .02). Aneurysms in the eight ruptured angiomyolipomas were all at least 5 mm in size and were 9 mm or larger in seven (88%). When aneurysm sizes of 5 mm or larger and 9 mm or larger were used for predicting rupture, sensitivity and speci- ficity, respectively, were 100% and 86% for the former criterion and 88% and 95% for the latter criterion.

A significant correlation was observed between aneurysm size and tumor size (P =0.003). the study concluded that aneurysm formation appears to be related to tumor size, and large aneurysms confer a higher probability of rupture.

MALIGNANT LESIONS

RENAL CELL CARCINOMA (RCC)

Renal cell carcinoma (RCC) is the most common adult renal epithelial cancer, accounting for more than 90% of all renal malignancies.[2]

RCC is the eighth most common malignancy affecting adults, accounts for between 3% and 4% of new cancer cases in the United States. It is the seventh most common cancer in men and the ninth most common in women [44]

The incidence in men is 1.6 times greater than in women. Metastatic disease at presentation varies with the patient series but typically occurs in about 1 in 10 patients. [45]

The classic clinical presentation of flank pain, hematuria, and a palpable flank mass is comparatively uncommon (5–10% of cases). However, clinical symptomatology may be quite nonspecific—for example, anorexia, tiredness, weight loss, or fever of unknown origin. Other presentations include varicocele formation (from tumor thrombus in the left renal vein or the inferior vena cava [IVC]) and disseminated malignancy.(46)

Most tumors present in the fifth to seventh decade of life, with a median age at diagnosis of 66 years and median age at death of 70 years. [47]

John g Doherty et al. [48] conducted a study to evaluate presentation, treatment and outcome of RCC in old age. 39 patients with diagnosis of RCC were identified. The mean age of the study group was 64.5 years(range 39 to 92 years). 25 were male. The population was divided into two groups - young group (<69 yrs)consisting of 29 subjects and old group (>70 years) consisting of 10. Seven tumors were identified incidentally while imaging for other indications. Anorexia, eight loss and abdominal pain were the most common symptoms in both groups.

Hypertension and anemia was also seen. The mean symptom duration was 9.9 weeks in both groups.The study concluded that neither clinical presentation, management nor survival differed between the young and elderly subjects.

Shalini Agnihotri et al. [49] conducted a study to investigate the spectrum of RCC in India with regards to age of onset, stage at presentation and survival. Of the total 617 renal tumours which were clinically suspected as RCC, 586 had epithelial cell tumour, the remaining 31 patients had non epithelial cell tumour. The mean size of the tumours was 8.08 ± 3.5 cm (median 7, range 1-25 cm). The mean age at diagnosis was 55.15 ± 13.34 (median 56, range 14-91) years. Overall, the proportion of patients presenting with clear cell carcinoma was 71.33 per cent. The study concluded that renal cell carcinoma was more frequent in younger people in India. One third of the patients were less than 50 yr of age and only 10.4 per cent patients had tumour of less than 4 cm (T1a). Younger patients of <39 yrs of age had a lower survival rates. Incidental detection of renal cell carcinoma (RCC) has increased with the mainstream use of abdominal computerized tomography (CT) and ultrasound. It has been demonstrated that incidentally discovered renal cell carcinoma (IRCC) tends to be smaller in size, of lower stage, and results in better survival outcomes than that of symptomatic RCC.(50)

The tumors are usually solitary but may be multifocal (6–25%), with bilateral RCC occurring sometime in the course of life in 4% of patients.

Paresh Jain [51] conducted a study to study the mode of presentation (incidental vs symptomatic) of renal cell carcinoma (RCC) with pathological prognostic factors. The pathological factors (tumor size, stage, grade, histopathological type) in relation to the mode of presentation were analyzed according to 1997 TNM criteria. 328 consecutive patients operated for clinically

suspected renal cell carcinoma were reviewed. 93 (28.4%) had incidental diagnosis and 235 (71.6%) had symptomatic presentation. Sex results and side of distribution was not significantly different in the two groups. Mean tumor size was 5.75 ± 2.73 cm in incidentally detected RCC (IRCC) and 9.32 ± 3.70 ($P < 0.001$) in symptomatic RCC (SRCC). Stage I and II tumors were signifi cantly greater in IRCC than SRCC. Whereas stage III and IV tumors were signifi cantly less in IRCC than SRCC. There was a predominance of higher grade tumors in SRCC, 50% being higher grades (Fuhrmanís grade III and IV) in SRCC than 28.1% in IRCC ($P = 0.003$). to conclude Incidental detection of renal carcinoma as compared to symptomatic tumors is lower in India as compared to western world. Incidental tumors have significantly favorable pathological prognostic factors.

RCC is associated with von Hippel-Lindau disease, hereditary papillary renal cancer, and, possibly, tuberous sclerosis.

The risk factors for RCC include cigarette smoking; obesity; diuretic use; exposure to petroleum products, chlorinated solvents, cadmium, lead, asbestos, and ionizing radiation; high-protein diets; hypertension; kidney transplantation; and HIV infection.

MDCT has been a major advance, providing angiographic and 3D imaging essential for presurgical planning. Three-dimensional CT helps delineate the precise location of the renal mass and its relationship to the surface of the kidney, the collecting system, and the renal vessels. The arterial and venous anatomy of the kidney is depicted at three dimensional CT angiography. (52)

Histologic subtypes according to the Heidelberg classification include clear cell ("conventional") adenocarcinoma (80%), papillary (15%), chromophobe (5%), collecting duct (1%), and unclassified (4%)

Clear Cell RCC

Previously referred to as conventional RCC, clear cell RCC is the most common histologic subtype, accounting for 70% of all RCCs. Clear cell RCC recapitulates the epithelium of the proximal convoluted tubules. The intracytoplasmic glycogen and lipids get dissolved during histologic processing, rendering the cells "clear". Lipid-rich cells in clear cell RCC impart the classic golden yellow colour at gross pathologic analysis. Clear cell RCC appears heterogeneous with areas of necrosis and hemorrhage. A profuse network of small, thin-walled sinusoid like blood vessels is a characteristic diagnostic feature.

Clear cell RCCs typically show hypervascularity on contrast-enhanced studies including computed tomography (CT. The degree of contrast enhancement may help distinguish clear cell RCC from non– clear cell variants. In a study that evaluated the helical CT findings of 76 clear cell RCCs, **Kim et al**. [16] found that clear cell RCC showed enhancement of more than 84 HU in the corticomedullary phase and 44 HU in the excretory phase (with a specificity of 100% and 91%, respectively.[53]

Jonathan R (2013) [36] conducted a study to determine whether enhancement at multiphasic multidetector computed tomography (CT) can help differentiate clear cell renal cell carcinoma (RCC) from oncocytoma, papillary RCC, and chromophobe RCC. 298 cases of RCC and oncocytoma were reviewed. Mean enhancement of clear cell RCCs and oncocytomas peaked in the corticomedullary phase; mean enhancement of papillary and chromophobe RCCs peaked in the nephrographic phase. Enhancement of clear cell RCCs was greater than that of oncocytomas in the corticomedullary (125 HU vs 106 HU, $P = .045$) and excretory (80 HU vs 67 HU, $P = .034$) phases. Enhancement of clear cell RCCs was greater than that of papillary RCCs in the corticomedullary (125 HU vs 54 HU, $P < .001$) , nephrographic (103 HU

vs 64 HU, *P* < .001), and excretory (80 HU vs 54 HU, *P* < .001) phases. Enhancement of clear cell RCCs was greater than that of chromophobe RCCs in the corticomedullary (125 HU vs 74 HU, *P* < .001) and excretory (80 HU vs 60 HU, *P* = .008) phases. Thresholding of enhancement helped to discriminate clear cell RCC from oncocytoma, papillary RCC, and chromophobe RCC with accuracies of 77% (83 of 108 cases), 85% (101 of 119 cases), and 84% (81 of 97 cases).

Calcification (sometimes ossification) is seen in 10%–15% of tumors. Larger renal masses tend to have more calcifications than small renal lesions. On CT, the calcifications of RCC may be punctate, amorphous, linear, or peripheral . (2)

Multilocular Cystic RCC [54]

Multilocular cystic RCC, as the name suggests, is a multiseptated cystic RCC whose septa contain small clusters of clear cells . Multilocular cystic RCC is found in adults aged 20–76 years with a mean age of 51 years. Males predominate with a male-to-female ratio of 3:1.

Multilocular cystic RCC is characterized by septated, variable-sized cysts separated from the kidney by a fibrous capsule.

On imaging Multilocular cystic RCC's typically manifest as multilocular cystic tumors. Asymmetric septal thickening may be seen. Twenty percent of tumors show septal or wall calcification.

Multilocular cystic RCC carries an excellent prognosis following nephrectomy. Recurrenceand metastasis have not been reported

Papillary RCC

Papillary RCC (chromophil RCC) is the second most common histologic subtype, making up 10%–15% of RCCs . Tumor epithelium is reminiscent of the

epithelium of the proximal convoluted tubules . Papillary RCC commonly affects end-stage kidneys.

Macroscopically, papillary RCCs often contain areas of hemorrhage, necrosis, and cystic degeneration (1) (Fig 9). Papillary RCC is histologically characterized by a predominantly papillary growth pattern. The tumor papilla consists of a fibrovascular core with stromal aggregates of foamy macrophages with cholesterol crystals.(2)

Papillary RCCs typically appear hypovascular and homogeneous on imaging studies. Papillary RCC typically shows lesser degrees of contrast enhancement than clear cell RCC at contrast-enhanced CT.

Another important feature of papillary RCC is that bilateral and multifocal tumors are more common than in other subtypes of RCC (especially with hereditary syndromes).

Kim et al. [53] report that these differences in enhancement peak in the corticomedullary phase. They found that clear cell RCC enhanced to a mean of 149 HU ± 46, whereas papillary RCC enhanced to a mean of 91 HU ± 12. The difference was less marked in the excretory phase, with clear cell RCC enhancing to a mean of 95 HU ± 17 and papillary RCC enhancing to 71 HU ± 10

Jinzaki et al. [55] further studied the MVD of various RCC subtypes and reported that the microvessel density of papillary RCC was less than that of clear cell RCC. They counted the number of microscopic vessels in a high-power field of a light microscope (×400; 0.1771 mm2 per field). clear cell RCC had the highest MVD at 653.6/mm2 ± 161.5, compared with only 110.7/mm2 ± 21 for papillary RCC. (55) At nonenhanced CT, calcification is seen slightly more often in pRCC than in cRCC. However, the presence or absence of calcification is not of value in making this differentiation.

Chromophobe RCC [54]

Chromophobe RCC is the third most common histologic subtype, accounting for less than 5% of RCCs . Chromophobe RCC shows a mean age of incidence in the 6th decade. Men and women are equally affected.

Chromophobe RCC appears uniformly hyperechoic at ultrasonography. Despite their large size, chromophobe RCCs demonstrate relatively homogeneous enhancement at CT and MR imaging . A spoke-wheel pattern of contrast enhancement classically associated with oncocytomas has recently been described in association with chromophobe RCC. Itis interesting to note that oncocytomas and chromophobe RCCs share similar ontogenic features, histologic features (on hematoxylin-eosin–stained slides), and some imaging findings. Renal vein invasionis seen in less than 5% of cases. Despite the overall favorable prognosis, large tumors may develop hepatic metastases.

Collecting Duct Carcinoma [54]

Collecting duct carcinoma of the kidney is a highly aggressive subtype of RCC that accounts for less than 1% of all malignant renal neoplasms. Collecting duct carcinoma shows a male-to-female ratio of approximately 2:1. The age range is 13–83 years (mean age, 55 years).

Collecting duct carcinoma typically appears as a gray-white infiltrative neoplasm with its epicenter in the pelvicaliceal system. Collecting duct carcinoma is histologically characterized by a constellation of findings such as tubular or tubulopapillary growth pattern, presence of inflammatory or desmoplastic stroma, and mucin production. Tubular epithelial dysplasia in the adjacent renal parenchyma is a characteristic histologic feature.

At CT, the mass appears hypoattenuating and hypovascular (9). Calcification is seen in up to 25% of patients.

Yuxiao HU [56] The purpose of the present study was to characterize the imaging features of CDC and improve its diagnosis. Radiological data of six cofirmed patients of collecting duct carcinoma were retrospectively reviewed with non-contrast computed tomography (CT) scans, five with contrast-enhanced CT scans, one with magnetic resonance urography, one with renal dynamic imaging and two with conventional whole-body ^{18}F-fluorodeoxyglucose (FDG) positron emission tomography (PET)/CT scans. seven tumors were detected in the six cases, with a mean size of 5.3 cm. Of the tumors, two were solid and the rest were complex solid and cystic. On non-contrast CT scanning, high, equal and low attenuation was observed in two, four and one tumors, respectively. In total, six tumors were located in medullary areas and only 1 tumor was found in the cortical location. A tiny calcification was present in only one tumor and cystic components were observed in five tumors, but no pseudocapsule was observed. Weak enhancements were observed in all six tumors examined with contrast-enhanced CT, and heterogeneous enhancements were also observed in the majority of these tumors with the exception of one tumor. An infiltrative pattern of tumor growth was present in five tumors, with an expansible appearance in the remaining two tumors.

Renal Medullary Carcinoma [54]

Renal medullary carcinoma, also referred to as the seventh sickle cell nephropathy, is an extremely rare malignant neoplasm occurring almost exclusively in patients withsickle cell trait.

Renal medullary carcinoma is hypothesized to arise from medullary collecting ducts. Renal medullary carcinoma is almost always found in young patients; the

typical age range is between 10 and 40 years (mean age, 22 years). The male to-female ratio is 2:1.

Renal medullary carcinoma appears a san infiltrative, heterogeneous mass with a medullary epi-center ,manifesting as an infiltrative, heterogeneous medullary neoplasm.

Hemorrhage and necrosis contribute to tumor heterogeneity. Renal medullary carcinoma is typically associated with caliectasis. Bimodal, lymphohematogenous metastases occur rapidly; the liver and lung are the most common target sites of metastasis.

Fuhrman histological grading system for renal cell carcinoma. [57]

Grade 1 Small (<10 microns) round hyperchromatic nuclei with inconspicuous nucleoli

Grade 2 Larger nuclei (15 microns) with open chromatin pattern; nucleoli are not visible at 10x but are identifiable at high magnification.

Grade 3 Large nuclei (20 microns)with open chromatin and prominent nucleoli. Readily visible even at low magnification.

Grade 4 Bizarre, pleomorphic or multilobed nuclei.

Staging of RCC

Staging systems are designed to reflect the modes of spread and are used to stratify treatment options and to assess prognoses and survival characteristics

TNM Staging of Renal Cell Carcinoma [58]

Stage Description

TX Primary tumor cannot be assessed

T0 No evidence of primary tumor

T1 Tumor < 7 cm in greatest dimension, limited to kidney

- T1a Tumor < 4 cm in greatest dimension, limited to kidney

- T1b Tumor > 4 cm but < 7 cm in greatest dimension, limited to kidney

T2 Tumor   7 cm in greatest dimension, limited to kidney

T3 Tumor extends into major veins or invades adrenal gland or perinephric tissues, but not beyond Gerota's fascia

- T3a Tumor invades adrenal gland or perinephric tissues but not beyond Gerota's fascia

- T3b Tumor grossly extends into renal vein(s) or vena cava below diaphragm

- T3c Tumor grossly extends into vena cava above diaphragm

T4 Tumor invades beyond Gerota's fascia

NX Regional lymph nodes cannot be assessed

N0 No regional lymph node metastasis

N1 Metastasis in a single regional lymph node

N2 Metastasis in more than one regional lymph node

MX Distant metastasis cannot be assessed

M0 No distant metastasis

M1 Distant metastasis

TNM Stage Groupings Stage Grouping

Stage I T1,N0,M0

Stage II T2,N0,M0

Stage III

- T1,N1,M0

- T2,N1,M0

- T3a,N1,M0

- T3b,N0,M0

- T3b,N1,M0

- T3c,N0,M0

- T3c,N1,M0

ROBSON Staging [(52)]

I – Confined to kidney

II – Within Gerota's fascia

III A – Renal vein or IVC invasion

III B – Lymph nodes

III C – Vascular invasion plus nodes

IV A – Direct organ invasion

IV B – Distant metastases

Tumor size is critical to staging RCC for tumors confined to the kidney. In patients with T1 stage classification of RCC, there is an overall improved survival in patients with tumors <4 cm comparedwith those whose tumors measure 4–7 cm. In a large study evaluating 47,909 cases from the National Cancer Database, patients with tumors <4 cm in diameter had a 75% 5-year survival rate, whereas tumors >10 cm in diameter yielded a median survival rate of 47.5% at 5 years.(59)

Klatte et al. [(60)] showed that 7% of patients with primary tumors <4 cm had metastatic disease at presentation in a series of 1067 patients. Locally aggressive stages (pT3a and above) have been reported in 5.6% to 8% of patients with RCCs <4 cm.

IMAGING EVALUATION OF RENAL CELL CARCINOMA [(46)]

American College of Radiology
ACR Appropriateness Criteria®

Clinical Condition: **Renal Cell Carcinoma Staging**

Radiologic Procedure	Rating	Comments	RRL*
CT abdomen without and with contrast	9	This procedure is complementary to x-ray chest.	☢☢☢☢
X-ray chest	8	This procedure is complementary to CT.	☢
MRI abdomen without and with contrast	8	This procedure is an alternative to CT.	O
CT abdomen with contrast	7	This procedure is an alternative to CT without and with contrast.	☢☢☢
CT chest without contrast	6		☢☢☢
CT chest with contrast	6		☢☢☢
CT abdomen and pelvis with contrast	5		☢☢☢☢
CT abdomen and pelvis without and with contrast	5	This procedure may be appropriate but there was disagreement among panel members on the appropriateness rating as defined by the panel's median rating.	☢☢☢☢
MRI abdomen without contrast	5		O
Tc-99m bone scan whole body	5		☢☢☢
MRI head without and with contrast	4		O
CT head with contrast	4		☢☢☢
CT abdomen and pelvis without contrast	3		☢☢☢☢
CT chest without and with contrast	3		☢☢☢
MRI head without contrast	3		O
CT head without contrast	3		☢☢☢
CT head without and with contrast	3		☢☢☢
US abdomen	3		O
FDG-PET/CT skull base to mid-thigh	3		☢☢☢☢
CT abdomen without contrast	2		☢☢☢
Rating Scale: 1,2,3 Usually not appropriate; 4,5,6 May be appropriate; 7,8,9 Usually appropriate			***Relative Radiation Level**

Computed Tomography

Computed tomography (CT) is a noninvasive imaging modality that uses ionizing radiation to characterize renal masses. Use of iodinated contrast material significantly improves the ability to characterize and stage the primary tumor and nodal and distant metastases. In general, 100–150 mL of iodinated intravenous (IV) contrast medium is used, with a flow rate of 2–3 mL/s. A noncontrast scan followed by a contrast-enhanced scan improves detection of small lesions in the kidney. Lack of soft-tissue contrast limits the sensitivity of CT scanning without IV contrast as a stand-alone examination.

Chest CT is useful to detect small pulmonary metastases and metastatic mediastinal lymph nodes. Use of IV contrast does not improve detection of intrathoracic metastasis.

CT scanning of the brain may be useful in detecting brain metastasis. Noncontrast CT scanning of the brain may not be effective in detecting lesions that are small or lack mass effect or significant vasogenic edema. Use of contrast increases the accuracy of CT scans of the brain.

Magnetic Resonance Imaging

MRI provides excellent soft-tissue contrast resolution and provides radiation-free multiplanar anatomic evaluation of the abdominal organs. MRI is generally used when optimal CT cannot be performed, as in the case of pregnancy or severe allergy to iodinated contrast medium. MRI is also useful in instances where there is equivocal contrast enhancement on CT or in instances of hemorrhagic lesions. MRI has similar reported overall staging accuracies compared with CT.

A MRI protocol for renal mass evaluation should include T2-weighted images, in- and opposed-phase T1-weighted gradient echo images to detect intravoxel fat, and

dynamic contrast-enhanced 3-D T1-weighted gradient echo images in arterial, nephrographic, and excretory phases.

Due to its superior contrast resolution, MRI of the brain is very useful in detecting brain metastasis and for detecting meningeal tumor seeding. Compared to CT, MRI is useful in detecting smaller lesions and lesions adjacent to the bones. Approximately 20% of patients who demonstrated a single lesion on CT demonstrated multiple lesions on MRI.[61]

Chest Radiography

Chest radiography uses ionizing radiation and is useful as a screening tool to detect pulmonary metastasis. Small pulmonary metastases are easily missed on chest radiographs. In high-risk patients, a chest CT is preferred.

Ultrasonography

Ultrasound (US) is an imaging modality free of ionizing radiation. US can be useful in differentiating solid and cystic renal masses. However, US is operator dependent and is challenging in obese patients who provide poor acoustic windows. Some of the challenges in the use of US may be related to incomplete visualization of the mass, acoustic shadowing from partially calcified cysts or masses, variability in echogenicity of hemorrhagic cysts, and poor sensitivity in diagnosing isoechoic small renal tumors. Hence, US is seldom used for local staging of RCC other than for clarification of potentially cystic tumors

Bone Scans

Tc-99m methylene diphosphonate bone scans provide a surveyof the entire skeleton to detect bone metastases. Bone scans involve injection of a radioisotope and use ionizing radiation. Bone scans are nonspecific in determining the cause of increased traceruptake, particularly in solitary lesions, and may occasionally require

an accompanying radiograph or cross-sectional imaging to further characterize the lesion. When available, singlephoton emission computed tomography fused with CT can be utilized to provide detailed anatomic localization of the abnormal radiotracer uptake and further improve the characterization of the nature of the abnormality.

They also have poor spatial resolution and contrast resolution. However, the ability to survey the entire skeleton at a relatively low cost and wide availability make it a useful tool in initial screening for bone metastasis.

Arteriography

Fluoroscopy and radiography are used while performing renal arteriography after inserting a catheter into the renal artery or the aorta for injection of contrast. It is an invasive procedure and is performed when therapeutic interventions at the same setting, such as embolization of the tumor, are planned. Diagnostic arteriography is rarely performed as a stand-alone procedure.

Fluorine - 18- 2- fluoro- 2- deoxy - D- glucose – positron emission tomography / computed tomography

Positron emission tomography (PET)/CT sequentially acquires PET scans and a CT scan, usually in a single system wherein both scanners are fitted into a single gantry. This enables the ability to provide coregistered images of both PET and CT scans. The most widely used tracer for PET scanning is fluorine-18-2-fluoro-2-deoxy-D-glucose (FDG), which is a positron emitter. PET/CT scanners involve exposure to ionizing radiation.

Fuccio C [62] conducted a retrospective study to assess the usefulness of F-FDG PET/CT in the restaging of clear cell renal cell carcinoma (RCC) patients. Sixty-nine patients (median age = 62 years; range = 36-86 years) affected by clear cell RCC underwent whole-body F-FDG PET/CT to restage the disease after nephrectomy for

clinical or radiological suspicion of metastases. On a lesion basis, PET/CT detected 114 areas of abnormal uptake in 42 positive patients of which 112 resulted to be true positive. FDG uptake of the true positive lesions resulted to be high in 83 cases, moderate in 17 lesions, and finally faint in 12 lesions. FDG PET/CT demonstrated a good sensitivity in the restaging of clear cell RCC.

Use of PET/CT is controversial in renal cell carcinoma. PET/CT appears to have a better sensitivity for detecting distant metastasis than for detecting and staging RCC in the kidney. PET/CT with 18F-sodium fluoride [46]

Transitional cell carcinoma

Urothelial cancers of the renal pelvis and collecting system constitute approximately 10%–15% of all renal tumors: 90% are transitional cell carcinoma (TCC), 9% are squamous cell carcinoma, and 1% are mucinous adenocarcinoma. Most tumors occur in the 6th and 7th decades of life, with males affected three times more often than females.[63]

The most important risk factor is smoking, with smokers being two to three times more likely to develop TCC than nonsmokers (3). Chemical carcinogens (aniline, benzidine, aromatic amine, azo dyes), cyclophosphamide therapy, and heavy caffeine consumption are also associated with TCC, and all predispose to synchronous and metachronous tumor development.[64]

Renal pelvic TCC occurs most frequently in the extrarenal part of the renal pelvis, followed by the infundibulocaliceal region.

Patients usually present with gross or microscopic hematuria, dull flank pain,or acute renal colic due to obstruction. Synchronous bladder cancer occurs in 2%–4% of patients with upper tract tumors; this is the reason for a full urothelial screening. Moreover, 40% of patients with upper tract TCC will develop

metachronous TCC of the lower urinary tract; this is the reason for bladder surveillance during follow-up of these patients.

Nocks BN et al. [65] studied sixty-eight patients with transitional cell carcinoma of the renal pelvis with respect to clinical presentation, tumor grade, stage and location, subsequent development of other urothelial tumors, and patient survival. Of the 66 patients with adjacent mucosa available for evaluation, 63 (95 per cent) had abnormal findings with severe dysplasia and Carcinoma In Situ common in the high-grade, high-stage tumors. Twenty-eight patients (41 per cent) had transitional cell carcinoma previously, concomitantly, and/or subsequently, and in 14 patients (21 per cent) subsequent bladder tumors developed.

On unenhanced CT scans, renal pelvic TCCs have soft-tissue attenuation; after intravenous administration of contrast material, these tumors show variable enhancement. Attenuation and enhancement characteristics help distinguish clot, tumor, and calculus; however, up to 2% of renal pelvic TCCs are calcified and thus may be difficult to distinguish from calculi. Tumour types cannot be reliably differentiated with CT, although renal cell carcinomas tend to enhance more than TCCs. Circumferential or eccentric mural thickening of the renal pelvis or ureter may be seen.

In addition, contrast-enhanced CT scans may demonstrate abnormalities in the renal parenchyma in cases of infiltrating TCC. A striated or delayed pattern is occasionally the result of such an infiltrating neoplasm, but ureteral obstruction and pyelonephritis may also cause this appearance and are more common than TCC. In the setting of diminished function of a kidney that is either obstructed or replaced by tumor infiltration, CT is more useful than urography because it can demonstrate the

tumor and its relationship to surrounding structures. Tumor invasion of the renal vein or inferior vena cava can occasionally be demonstrated by CT [66]

Twenty-two patients with a pathological diagnosis of transitional-cell carcinoma of the ureter or renal pelvis underwent a preoperative CT examination. 7 had post-contrast scans only. Nineteen patients had a solitary lesion and 3 had multiple lesions. There was 1 lesion involving the calyx, 8 involving the renal pelvis, 6 intrarenal, and 9 ureteral. There was 1 lesion involving the calyx, 8 involving the renal pelvis, 6 intrarenal, and 9 ureteral. Three distinct CT patterns were seen - Intraluminal Mass in 12 cases: Attenuation values of the tumors approximated that of muscle (40-68 H) in 11 and calcium in 1. Of 9 patients studied with both pre and post-contrast scans, only one exhibited contrast enhancement: the density of the tumor increased from 49 H on pre-contrast scans to 78 H on post-contrast scans. Ureteral Wall Thickening in 5 cases: In these patients ureteral wall thickening was diffuse and symmetrical, causing circumferential narrowing of the lumen. In 1 case, focal thickening of the ureteral wall was also noted at different levels, resulting in a semilunar appearance. The attenuation values of the thickened ureteral wall approximated that of soft tissue. Infiltrating Renal Mass in 7 cases: Seven lesions presented as infiltrating renal masses indistinguishable from other intrinsic renal tumors. Six were subsequently shown to be local or direct metastases (spread) from a calyceal/pelvic transitional-cell carcinoma.[67]

TNM Classification of Renal TCC [68]

Tx Primary tumor cannot be assessed

T0 No evidence of a primary tumor

Ta Papillary noninvasive carcinoma

Tis Carcinoma in situ

T1 Tumor invades subepithelial connective tissue

T2 Tumor invades the muscularis

T3 Tumor invades beyond the muscularis into the periureteric fat or renal parenchyma

T4 Tumor invades adjacent organs, the pelvic or abdominal wall, or through the kidney into perinephric fat

Nx Regional lymph nodes cannot be assessed

N0 No regional lymph node metastasis

N1 Metastasis in a single lymph node   2 cm in greatest dimension

N2 Metastasis in a single lymph node >2cm but   5 cm in greatest dimension or in multiple lymph nodes.

N3 Metastasis in a lymph node >5 cm in greatest dimension

Mx Distant metastasis cannot be assessed

M0 No distant metastasis

M1 Distant metastasis

The ability to obtain thin slices with helical CT and MDCT has vastly improved the ability of CT to assess urothelial tumors. Apart from the advantages of CT to inspect the urinary tract in multiple planes and to assess for periureteric and renal infiltration, CT permits assessment of nodal and distant metastases, thus providing both urothelial and metastasis surveillance in a single examination.

METASTASES

Renal metastases are present in approximately 10% to 20% of patients, depending on tumor type. The most common primary sites for renal metastases include lung, colon, and breast carcinoma; melanoma; and reproductive organ malignancies such as testicular or ovarian carcinoma. Melanoma, when present,

frequently metastasizes to the kidneys, but it is less common than the other types of primary malignancies.

CT is very sensitive for renal metastases. The most common appearance of renal metastatic disease is usually multifocal small renal masses and they may involve both kidneys. Renal metastases are typically hypodense and do not commonly demonstrate hyperenhancement. The lesions measure 20 to 40 HU on nonenhanced CT images and have minimal enhancement after intravenous contrast of 5 to 15 HU. Invasion of the perinephric space by a renal metastasis is seen in metastases from melanoma or lung carcinoma. This type of perirenal metastatic disease usually represents lymphatic spread. Diffuse infiltrative metastases may also occur. Hemorrhagic renal metastases are most closely associated with melanoma primaries but may occur with other primaries, such as pheochromocytomas and leiomyosarcomas.

Solitary metastasis may resemble RCC, but RCC typically has more necrosis. Other findings, such as hyperenhancement and renal vein thrombosis, help suggest RCC over metastasis.

Infectious Renal Pseudotumors

Focal Pyelonephritis [16]

Renal infection confined to a single lobe is called focal pyelonephritis . Renal infection involving multiple lobes of the kidney is referred to as multifocal pyelonephritis. It is more common in patients with diabetes and those who are immunocompromised. Patients typically present with flank pain, fever with chills, and pyuria. Focal pyelonephritis is seen on sonography as either a hypoechoic or hyperechoic lesion in the renal cortex extending from the renal medulla to the renal capsule, with decreased perfusion on color-flow Doppler imaging. CT shows a focal

wedge shaped area of low attenuation without a well defined wall around it, and without an overlying bulge on the renal surface, which distinguishes it from renal cell carcinoma. Striations may also be observed in the nephrogram. Extension of the acute inflammatory process into the perirenal soft tissues may give the appearance of a renal malignancy. Someinfiltrative renal tumors (particularly medullary renal carcinoma) may have an appearance similar to that of focal pyelonephritis. In such cases, clinical information can be helpful in making a diagnosis.

Renal abscess[16]

Renal abscesses are primarily caused by an ascending infection from the lower urinary tract with gram-negative bacilli and enteric bacteria. Renal abscesses are primarily caused by an ascending infection from the lower urinary tract with gram-negative bacilli and enteric bacteria. Sonography and CT reveal a well-defined heterogeneous mass that at times may simulate a renal malignancy. Features such as irregular walls with increased through-transmission on sonography and a low-attenuation lesion with enhancing walls on CT, along with a history of fever and a positive urinalysis and culture, indicate a renal abscess. Differentiation from a renal malignancy may be difficult if clinical information does not support the presence of infection. Pathologically, renal abscess is identified by the presence of pus and debris with varying degrees of reactive inflammatory changes.

Balfe et al. [69] reviewed sixty-six patients with an indeterminate CT diagnosis. The scans were reviewed retrospectively by two radiologists and patients were excluded if a definite diagnosis seemed possible after all. For this reason, 3 angiomyolipomas and 3 benign cortical nodules (pseudotumors) were excluded. In the 60 remaining cases (7.6%), review of the excretory urograms, retrograde pyelograms, angiograms, sonograms, and CT scans was performed by three authors. The clinical

records, surgical findings, and pathological information for each patient were reviewed and follow-up information obtained from the referring physician. Lesions were categorized as (a) technically indeterminate, (b) cyst-like, or (c) solid with complex features. 26 cyst like masses were identified. Cyst like CT features were seen in majority with inconsistent features such as thickened wall , peripheral calcification, an attenuation value higher than that of a typical benign cyst (30-60 H), and/or an irregular contour or poor delineation from the surrounding normal tissue. Eighteen of these patients had surgery or needle aspiration, the most common diagnosis was a "complicated" cyst (hemorrhagic/ infected) in 14 cases, Abscess in 2, Benign neoplasm in 2, Metastasis in 2, Malgnant neoplasm in 2 and a Multilocular cyst. 8 masses were classified as Solid Masses with Complex Features. While they bore some resemblance to renal neoplasms, unusual features made that diagnosis uncertain. These included (a) involvement of the perinephric space disproportionate to the size of the mass, (b) extravasation of contrast medium or fresh hemorrhage into the perirenal tissues, and (c) a clinical presentation suggesting a non-neoplastic process, including fever, renal calculi, recent trauma, and/or young age. Seven of the patients had surgical confirmation. Four had xanthogranulomatous pyelonephritis and 3 had renal neoplasms (2 transitional-cell carcinomas and 1 renal-cell carcinoma) with extensive perirenal hemorrhage or urinoma formation.

Morehouse et al. [70] reviewed 40 patients with urinary tract inflammation. The study included 31 female and nine male patients ranged in age from 2 to 82 years. Twelve patients had diabetes mellitus, nine had renal stones, and 16 others had other risk factors, including urinary tract obstruction, trauma, history of intravenous drug abuse, or a debilitating disease. Of the 38 patients, 34 had fever, 26 had an elevated white blood cell count greater than 10,000, and 31 had an abnormal urinalysis.

Positive urine cultures were obtained in 29 patients. Six patients with focal pyelonephritis were diagnosed by sonography or CT. In all of these cases, a renal mass or defect in the nephrogram was evident on excretory urography. A hypoechoic mass with no through-transmission was found on sonography in each patient. CT was performed in five of these patients. Segmental areas of decreased attenuation with striations in the area of the mass were demonstrated on contrast-enhanced scans in four of these patients. Thickening of the fascial planes around the kidney was also apparent in all five patients. 17 renal abscesses were identified in 14 patients. Each of these patients had evidence of a mass on excretory urography. On CT, an area of decreased attenuation that did not enhance after intravenous contrast material was demonstrated in all 17 abscesses. In six of these, an enhancing rim around the mass was detected on the contrast-enhanced scan, and in three gas was present.

STATISTICS

The statistical analysis was done using IBM SPSS ver 20. The descriptive data for gender, enhancement characteristics, location and distribution of lesions was calculated. Chi square test was used to assess the association between subtype of renal masses (benign or malignant) and gender, morphological features, and type of contrast enhancement. To assess the association between benign and malignant masses with respect to age, size of lesion, contrast enhancement in corticomedullary and nephrographic phases student T test was used. The diagnostic efficacy and cut off values of enhancement and degree of enhancement in various phases was determined by reciever operating characteristic (ROC) curve. The curves were analysed for cut off values to differentiate RCC from other masses. In all our analysis p value < 0.05 was significant.

RESULTS

The present study is a cross sectional study including 30 patients who had renal masses which was detected on MDCT between July 2014 - June 2016.

Table 1 - Age Distribution of Renal Masses

Renal masses	AGE in years
Mean	53.40
Std. Deviation	12.746
Minimum	26
Maximum	82

Table 2 - Sex Distribution Of Renal Masses

Sex distribution in renal masses	Frequency	Percent
MALE	19	63.3
FEMALE	11	36.7
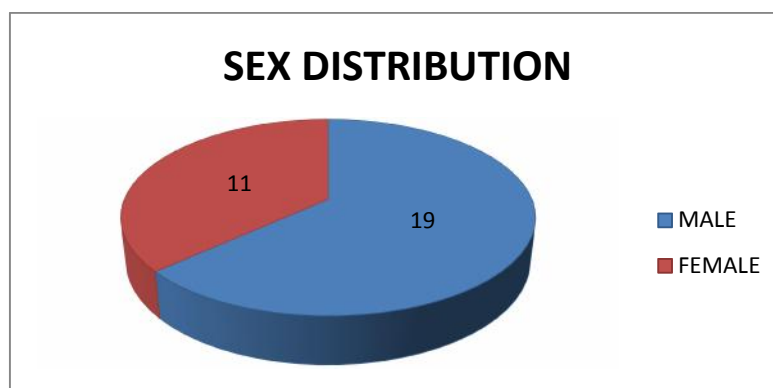
In this series the mean age of patients was 53 ± 12 years (range 26 to 82 years) which include 19 males and 11 females.

Table 3 - Mode of presentation of renal masses

Symptoms present	Pain	Lump	Fever	Hematuria	Weight loss
Renal masses (no of cases)	24	6	8	6	11
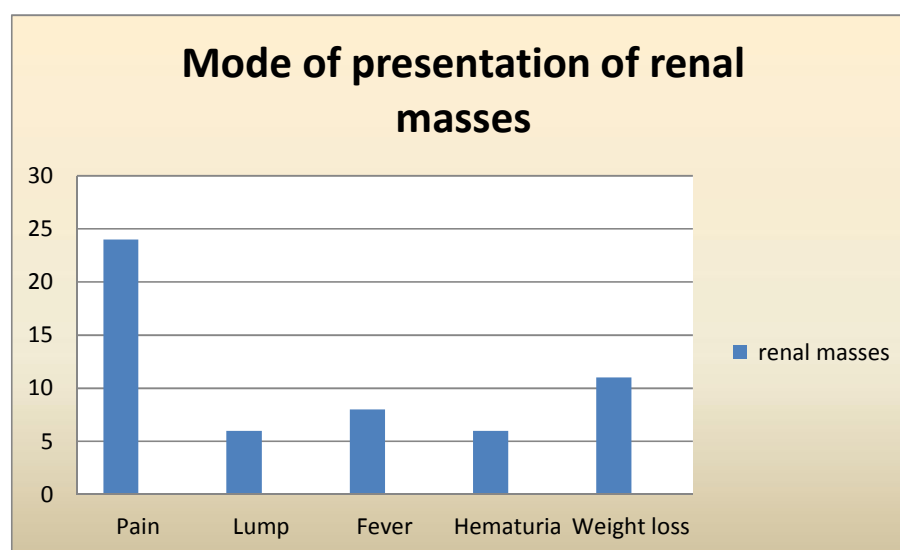
Most common of presentation of renal masses in our setting was dull aching pain which was seen in 25 cases (83 %), followed by weight loss in 10 cases (33 %), fever in 8 (26.7%), hematuria and lump in 6 (20%).

Most common of presentation in cases of renal cell carcinoma was pain in 12 cases (92 %), followed by weight loss in 8 (61.5%), hematuria in 4 (30.8%) and fever in 2 (15.4 %). hemoglobin levels were decreased in 7 cases (46.2 %).

The classic triad of flank pain, hematuria, and flank mass was seen in 2 cases (15.3%) of renal cell carcinoma.

Table 4 - Size of Renal Masses

Renal masses	Size in cm
Mean	5.463
Std. Deviation	3.5744
Minimum	2.0
Maximum	18.0

The mean size of renal masses was 5.463 ± 3.5744 (range 2 to 18 cm)

Table 5 - Laterality of Renal Masses

	Frequency	Percent
RIGHT	13	43.3
LEFT	16	53.3
BILATERAL	1	3.3
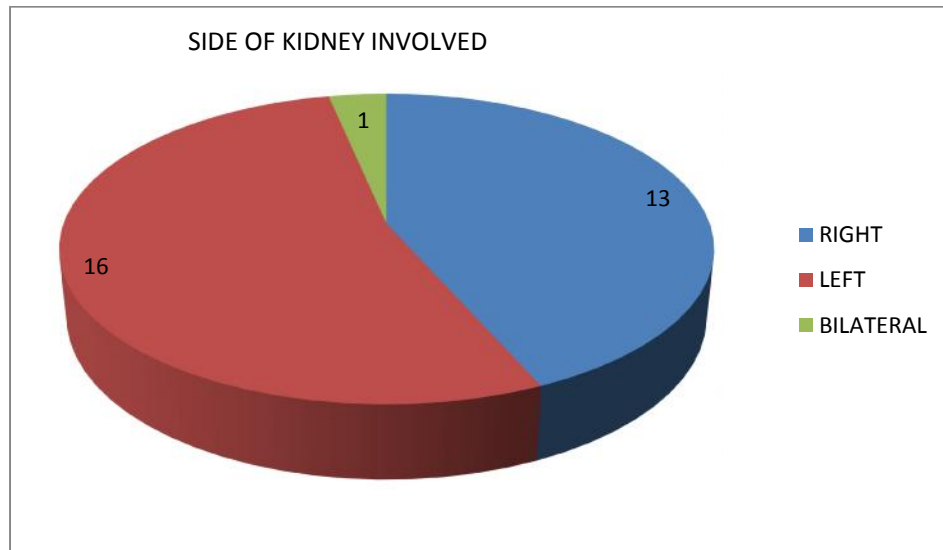
Right kidney was involved in 13 (43.3 %), left in 16 (53.3 %) and bilaterally in one (3.3 %) cases. There were 34 lesions in 30 patients, a single lesion was noted in 27 cases, and two lesions were detected in each case of AML and renal abscess and three lesions in a case of renal abscess which was located bilaterally.

Table 6 - Location Of Renal Masses

Location	No of cases
Upper pole	8
Interpole/midpole	4
Lower pole	5
Whole kidney	3
Upper and midpole	4
Mid and lower pole	4
Upper and lower pole	2
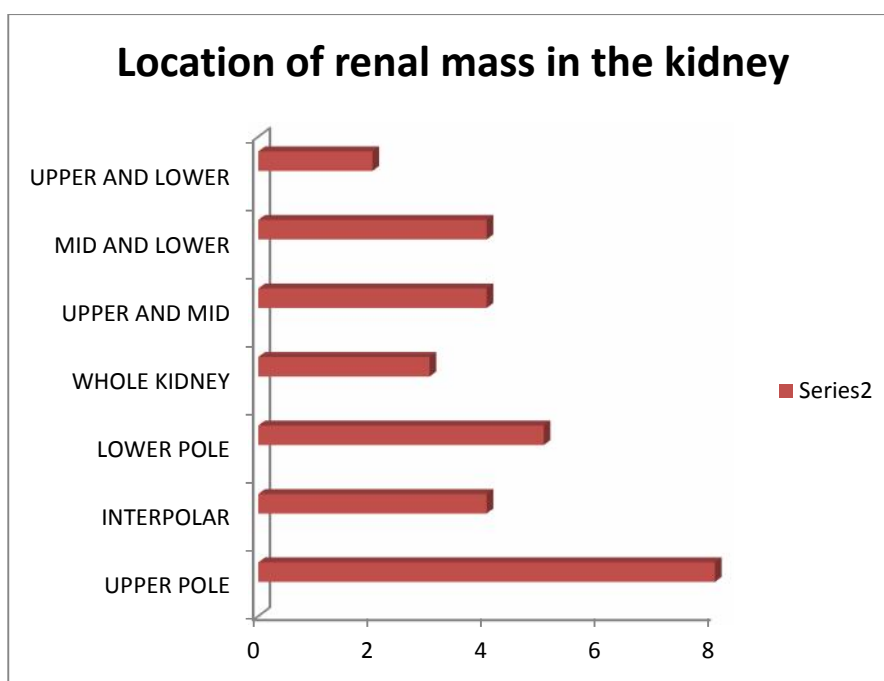
Right kidney was involved in 13 (43.3 %), left in 16 (53.3 %) and bilaterally in one (3.3 %) cases. There were 34 lesions in 30 patients, a single lesion was noted in 27 cases, and two lesions were detected in each case of AML and renal abscess and three lesions in a case of renal abscess which was located bilaterally.

Table 7 - Distribution of Cases as Benign/Malignant.

NATURE OF MASS	No of cases	Percent
BENIGN	14	46.7
MALIGNANT	15	50.0
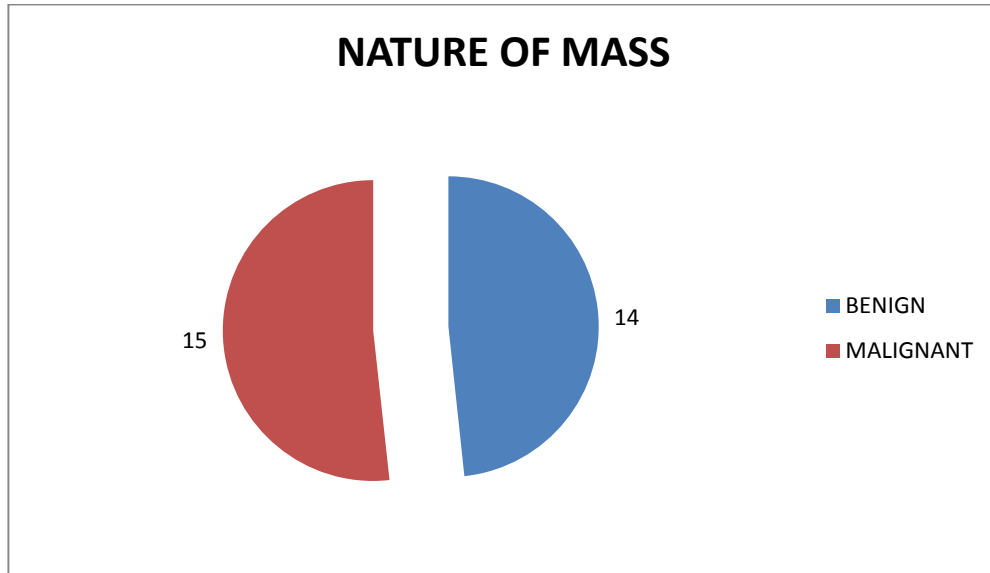
Out of a total of 30 cases renal masses, 14 cases were benign and 15 were malignant masses

Table 8 - Distribution of Cases.

Diagnosis	No of cases	Percent
TCC	1	3.3
RCC	13	43.3
RENAL ABSCESS	7	23.3
AML	4	13.3
BOSNIAK TYPE II CYST	2	6.7
BOSNIAK TYPE III CYST	1	3.3
RENAL METASTASIS	1	3.3
ONCOCYTOMA	1	3.3

Chart Title

■ Frequency

TCC	1
RCC	13
RENAL ABSCESS	7
AML	4
BOSNIAK TYPE 2...	2
BOSNIAK TYPE III	1
RENAL METASTASIS	1
ONCOCYTOMA	1
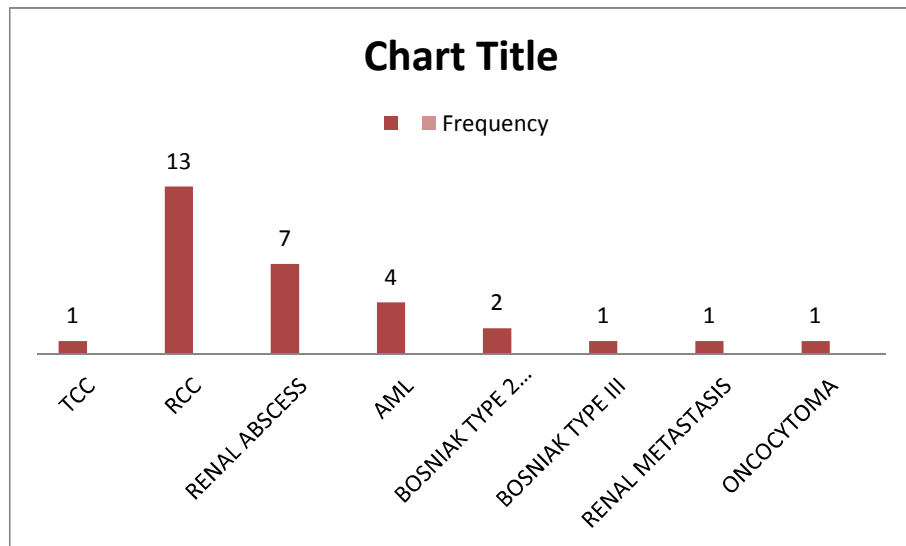
Table 9 - Distribution of benign masses.

DISTRIBUTION OF BENIGN MASSES	No of cases	Percent
INFECTION	7	50.0
AML	4	28.6
BOSNIAK TYPE II CYST	2	14.3
ONCOCYTOMA	1	7.1
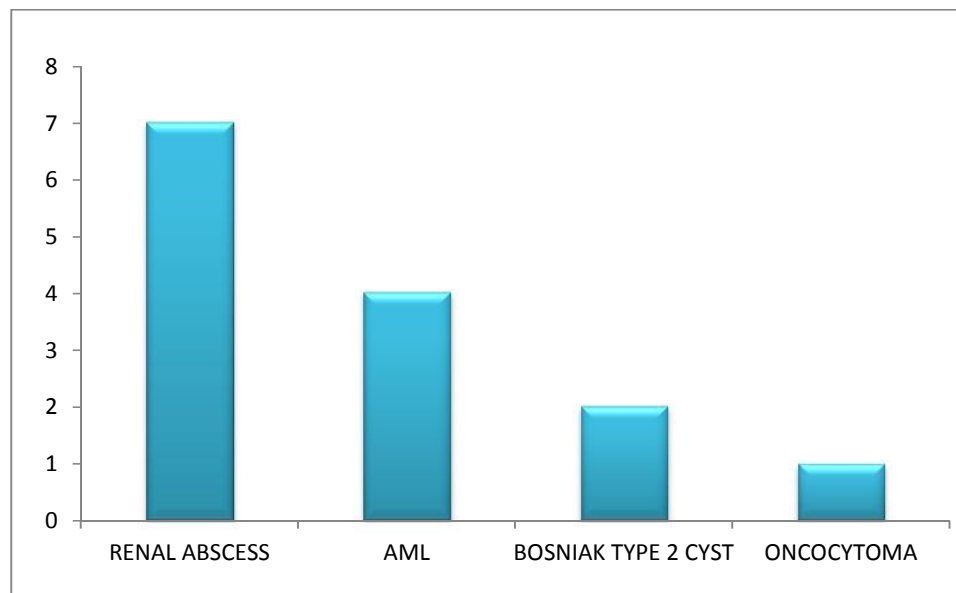
Table 10 - Distribution of malignant masses.

DISTRIBUTION OF MALIGNANT MASSES	No of cases	Percent
TCC	1	6.7
RCC	13	86.7
RENAL METASTASIS	1	6.7
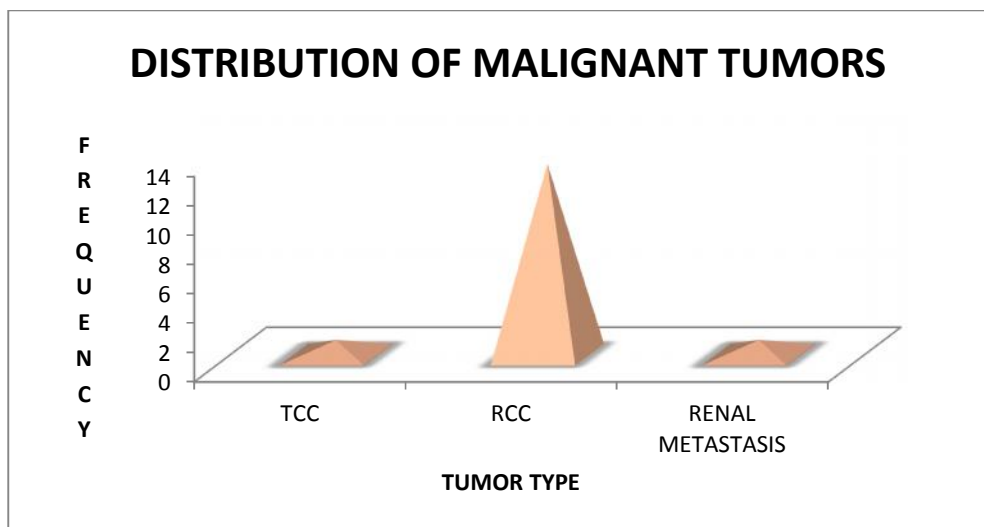
Out of a total of 30 cases renal masses, 14 cases were benign and 15 were malignant masses. The beingn lesions included 6 cases of renal abscess, 4 angiomylipoma, one oncocytoma and 2 cases of bonsniak type 2 cyst. Among malignant masses, 13 out of 15 cases were renal cell carcinoma among which 2 cases presented as a solid cystic mass with enhancing soft tissue densities and these were diagnosed as Bosniak type 4 cyst based on imaging findings, later these lesion turned out to be RCC on biopsy. One case was transitional cell carcinoma of renal pelvis. A metastasis (adenocarcinoma) from unknown primary was wrongly diagnosed as RCC on imaging. One case was diagnosed as Bosniak type III lesion however this case was lost in follow up and pathological report was not available.

Table 11 - Enhancement of normal renal cortex.

Enhancement of normal cortex	Mean HU	Std. Deviation
Unenhanced phase	32.06	3.83211
CMP	122.46	15.08307
NP	137.80	9.707
Degree of enhancement in CMP	90.40	16.04219
Degree of enhancement in NP	105.73	10.91324

The renal cortex demonstrated a mean attenuation of 32 ± 3 HU on unenhanced CT images. Cortical mean enhancement was 122 ± 15 HU during corticomeduallary phase and 137 ± 9 HU during nephrographic phase. the degree of enhancemnt in corticomedullary and nephrographic phases were 90 ± 16 and 105 ± 10. There was a statically significant difference in enhnancement in corticomedullary and nephrographic phase ($P < .05$).

Benign versus Malignant masses

Table 12 - Association between age and nature of renal masses.

Nature of renal mass	Mean age in years	Std. Deviation
BENIGN	45.71	11.605
MALIGNANT	61.13	9.125

The mean age among cases with malignant lesion was 61.13 years (± 9.12) and in cases with benign masses was 45.71 years (± 11.6). The association between age and renal masses was significant.

Table 13 - Association between gender and nature of renal masses.

	MALE	FEMALE
BENIGN	7	7
MALIGNANT	11	4
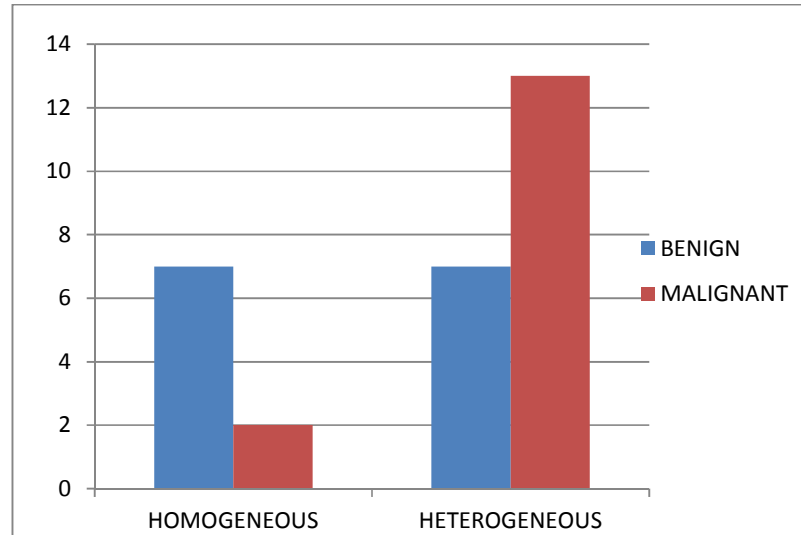
Benign masses were seen in 7 males and 7 females and malignant masses in 11 males and 4 females. Though malignant lesions were more commonly seen in males, the association between gender and malignant / benign masses was statistically insignificant with P >0.05

Table 14 - Comparison of size in benign and malignant renal masses

	Mean SIZE in cm	Std. Deviation
BENIGN	5.600	4.4037
MALIGNANT	5.567	2.7515

The mean size of benign masses was 5.6 cm and of malignant masses was 5.5 cm. the variability in size between malignant and benign masses was statistically insignificant (p > 0.05)

Table 15 - Mode of presentation in benign and malignant masses

Symptoms present (no of cases)	Pain	Lump	Fever	Hematuria	Weight loss
Benign renal masses	11	2	6	1	1
Malignant renal masses	13	4	2	5	10
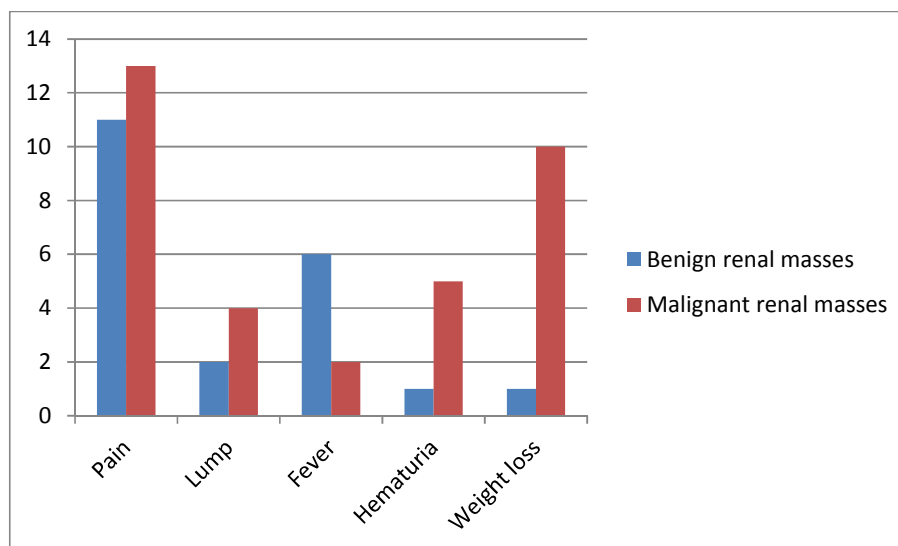
Hematuria was present in 5 out of 15 cases among malignant masses and in one out of 14 cases among benign masses. The association between them was insignificant p >.05

Pain was the most common symptom among benign and malignant masses. it was present in 11 out of 14 benign cases and 13 out of 15 malignant cases. the association between pain and type of renal mass of insignificant. (p .564)

2 out of 14 benign masses presented with lump where as 4 out of 15 malignant masses presented with lump. the association between them was insignificant with P >0.05.

6 out of 14 cases with benign masses presented with fever where as only 2 cases with malignant mass presented with fever. p.075

Weight loss was a significant symptom among patients with malignant renal masse. it was resent in 9 out of 15 cases. it was present only in 1 out of 14 cases with benign masses. the association between malignant masses and weight loss was statistically significant p <0.05

RADIOLOGICAL FEATURES OF BENIGN AND MALIGNANT LESIONS

Table 16 - Enhancement pattern in benign and malignant lesions

ENHANCEMENT PATTERN	HOMOGENEOUS	HETEROGENEOUS
BENIGN	7	7
MALIGNANT	2	13
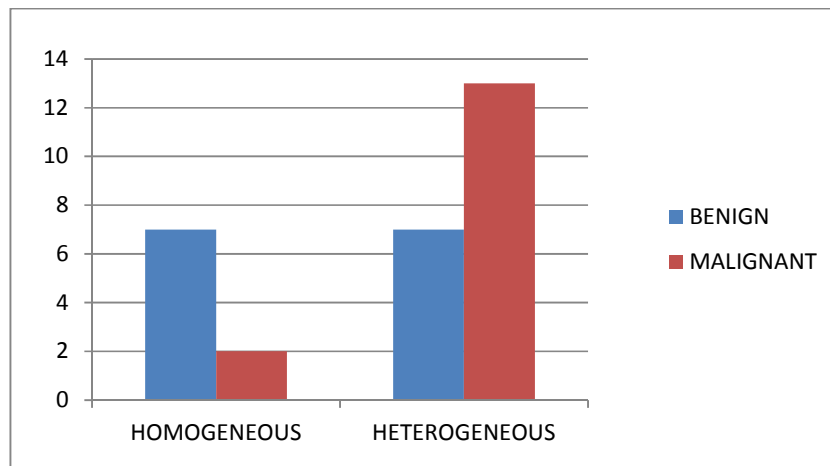
The enhancement pattern among benign renal masses was homogenous in 7 cases and heterogenous in 7. Among malignant masses 13 out of 15 cases enhanced heterogenously and only 2 cases were homogenous. the variability in enhancement pattern between benign and malignant lesion was significant with p value <0.05

Table 17 - Tumor margin in benign and malignant lesions

TUMOUR MARGIN	WELL DIFINED	ILLDEFINED
BENIGN	12	2
MALIGNANT	7	8
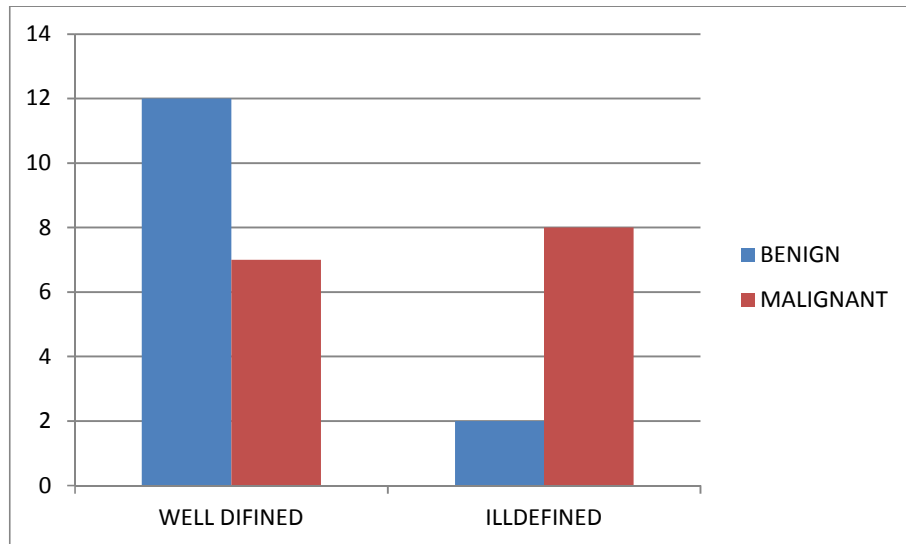
The benign masses were well defined in 12 out of 14 cases and ill defined in 2. the malignant masses were well defined in 7 out of 15 cases and ill defined in 8. the association between tumour margin and benign/malignant mass was significant $p < 0.05$

Table 18 - Calcification in benign and malignant lesions

CALCIFICATION	PERIPHERAL CALCIFICATION	ABSENT
BENIGN	4	10
MALIGNANT	0	15
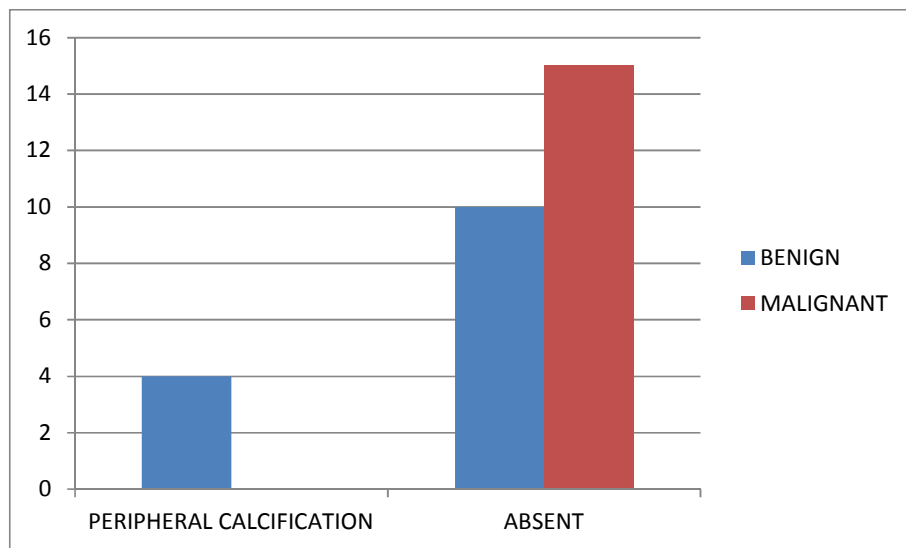
Peripheral calcification was seen in 4 out of 14 cases among benign masses where as malignant lesion did not show evidence of calcification.

Table 19 - Density in benign and malignant lesions

Non contrast CT	BENIGN	MALIGNANT
HYPODENSE	13	13
ISODENSE	1	1
HYPERDENSE	0	1
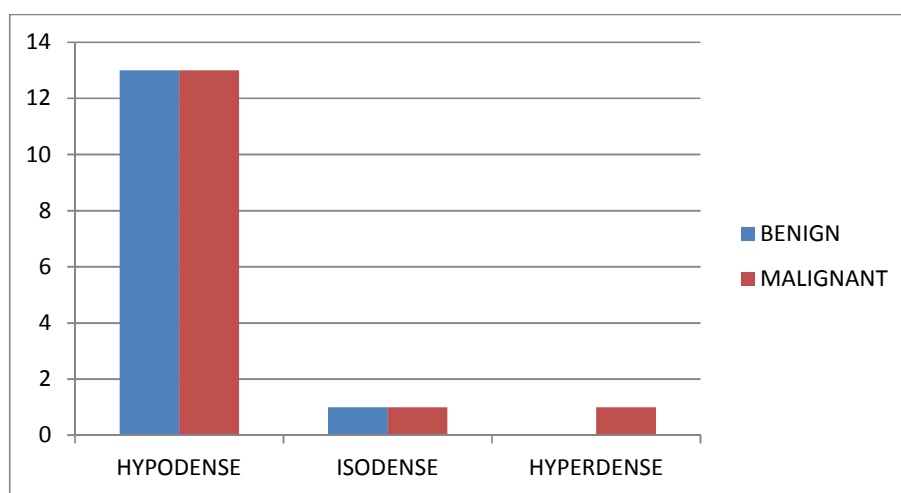
13 out of 14 benign cases presented as hypodense masses and one was isodense to renal cortex. 13 out of 15 malignant masses presented as hypodense masses and one cases each presented as isodense and hyperdense masses.

Table 20 - Attenuation In Pre And Post Contrast Ct Images In Benign And Malignant Lesions

	BENIGN	MALIGNANT
Unenhanced phase	9.29 ± 21.51	34.87 ±3.54
CMP	14.21± 26.76	96.53±12.97
NP	16.14±27.84	72.93±10.19
Degree of enhancement in CMP	4.9286 ±11.40	61.6667±15.29
Degree of enhancement in NP	6.8571±14.21	38.0667±10.85

The HU of renal masses were compared between benign and malignant masses in unenhanced and enhanced phases. In unenhanced sequences the benign masses showed a mean HU value of 9.29, the malignant masses showed a mean HU value of 34.87. In corticomeduary and nephrographic phases the mean HU in bening masses was was 14.21 and 16.14 respectively. the malignant masses displayed rapid enhancement and washout in corticomedulary and nephrographic phases with a mean HU value of 96.53 and 72.93 respectievely. the malignant masses showed greater mean enhancement in corticomedullary phase than in nephrographic phase. In contrary the benign masses - oncocytoma showed greater enhancement in nephrographic phase than in corticomedullary phase. The mean enhancement in different phases of enhancement and unenhanced phases between benign and malignant masses were statistically significant with p value <0.05.

RENAL CELL CARCINOMA

A total of 13 cases of renal cell carcinoma was included in my study (table10). It was the most common malignant mass lesion comprising of 86.7 % of the malignant mass lesions detected in my study. Two renal masses presented as a solid cystic mass with enhancing soft tissue components with no evidence of metastasis or renal vessel involvement. These masses were diagnosed as Bosniak type IV cysts based on imaging findings. The lesions turned out to be renal cell carcinoma on biopsy. One mass was diagnosed renal cell carcinoma based on enhancement >20 HU on corticomedullary and nephrographic phases. On biopsy the mass lesion was diagnosed as metastasis (adenocarcinoma) from an unknown primary.

Table 21 - Age And Size Distribution In RCC

Renal cell carcinoma	AGE in years	SIZE in cm
Mean	60.77	6.000
Minimum	50	2.1
Maximum	82	13.0

The mean age of patients with RCC was 60.77 years (range 50 to 82 years). The mean size of the RCC was 6 cm with a range of 2.1 to 13 cm.

Table 22 - Age group Distribution In RCC

Age groups	Frequency	Percent
41-50 years	1	7.7
51-60 years	7	53.8
61-70 years	3	23.1
>70 years	2	15.4
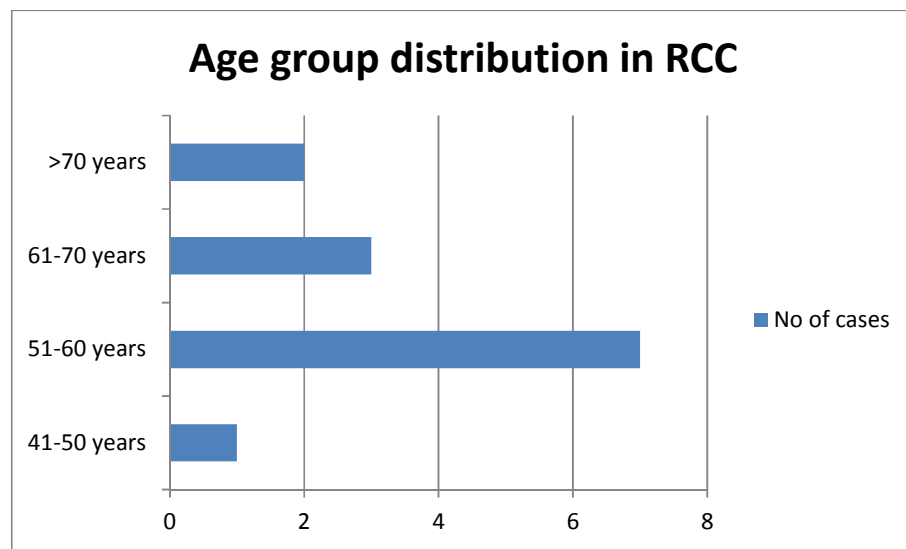
Most cases of RCC were seen in the age group of 51 to 60 years in 7 out of 13 cases followed by 61 to 70 years in 3, above 70 years in 2, and 41to 50 years in one.

Table 23 - Sex Distribution in RCC

Sex Distribution in RCC	Frequency	Percent
MALE	9	69.2
FEMALE	4	30.8

Out of 13 cases of RCC, 9 cases were seen in males and 4 in female,

Table 24 - Side Distribution in RCC

Laterality in RCC	Frequency	Percent
RIGHT	7	53.8
LEFT	6	46.2

There was almost equal distribution of cases in right and left kidneys. The right kidney was involved in 7 cases (53.8 %) and left in 6 (46.2 %). The upper pole and inter polar regions (6 out of 13 cases) were more commonly involved.

RADIOLOGICAL CHARACTERISTICS OF RCC

Table 25 - Enhancement pattern of RCC

Enhancement pattern	HOMOGENOUS	HETEROGENOUS
RCC	1	12

Heterogenous enhancemt was seen in 12 out of 13 cases of RCC and homogenous in one case.

Table 26 - Density of RCC

Density	HYPODENSE	ISODENSE
RCC	12	1

Out of the 13 cases of RCC'S, 12 masses were hypodense and the other was isodense

Table 27 - Tumour margin of RCC

Tumor margin	WELL DIFINED	ILLDEFINED
RCC	6	7

The RCC masses were well defined in 6 out of 13 cases of RCC and illdefined in 7 cases

Table 28 - Pre and post contrast attenuation of RCC

	Mean HU	Std. Deviation	Minimum	Maximum
Unenhanced phase	34.31	2.250	28	37
CMP	99.54	9.955	78	112
NP	72.23	10.810	56	95
Degree of enhancement in CMP	65.2308	10.61566	45.00	79.00
Degree of enhancement in NP	37.9231	11.54312	21.00	61.00

The 13 cases of RCC had a mean attenuation value of 34.31 ± 2.2 HU on a unenhanced scan with a range of 28 to 37 HU. all cases of RCC showed significant contrast enhancement after intravenous contrast injection. the mean attenuation value was maximum in corticomedullary phase followed by nephrographic phase (mean attenuation value in corticomedullary phase was 99.54 ($\pm$ 9.12) and in nephrographic phase was 72 ($\pm$ 10.8), the degree of enhancement in corticomedullary phase was 65.23 ($\pm$ 10.6) and in nephrographic phase was 37.9 ($\pm$ 11.54). Overall a pattern of enhancement detected in all cases of RCC in was rapid enhancement in corticomedullary phase followed by rapid washout in nephrographic phase. There was a significant deference between HU in corticomedullary phase and nephrographic phase in cases of RCC.

Table 29 – Area under the curve values in cases of RCC in pre and postcontrast images

	Area under the curve	Asymptotic Sig.b
Unenhanced phase	.916	.000
CMP	.991	.000
NP	.857	.001
Degree of enhancement in CMP	.989	.000
Degree of enhancement in NP	.835	.002

Diagonal segments are produced by ties.
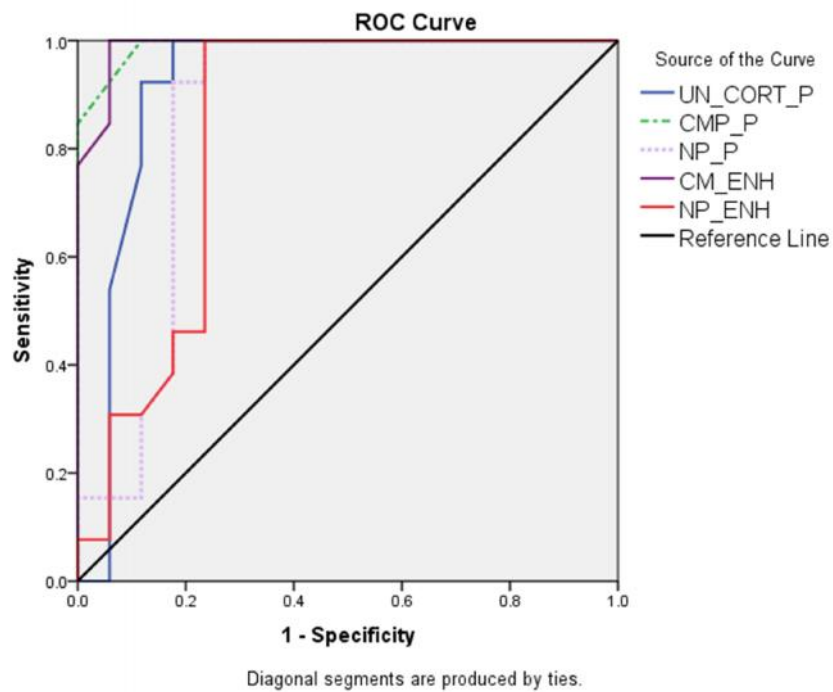
Reciever operating characteristic curves were analysed to evaluate attenuation values pre and post contrast to distinguish renal cell carcinomas from other renal masses. The area under the curve was maximum for corticomedullary phase with value of 0.991, which was statistically significant. The area under the curve for degree of contrast enhancement in corticomedullary and nephrographic phases were 0.989 and 0.835 respectievely, nephrographic phase 0.857, unenhanced phase was 0.916. all the above test variables were statically significant.

The roc curve analysis showed that the cut off values with highest sensitivity and specificity for characterization of RCC from other masses was 71.5 HU in corticomedullary phase (sensitivity   100%   , specificity 99.9%), 41.5 HU in nephrographic phase (sensitivity 100%   , specificity 99.8 %), degree of enhancement in corticomedullary phase was 44.5 (sensitivity   100%   , specificity 99.9%) and degree of enhancement in nephrographic phase was 15.5 (sensitivity   100%   , specificity 99.8%)

BENIGN CYSTIC LESIONS

Table 30 - Age distribution and enhancement of Benign cystic lesions

	Mean	**Std. Deviation**
AGE	46.00	16.971

	Mean HU	**Std. Deviation**
Unenhanced phase	15.00	1.414
CMP	16.50	2.121
NP	17.00	1.414
Degree of enhancement in CMP	1.5000	3.53553
Degree of enhancement in NP	2.0000	2.82843

Two radiologically benign cysts of Bosniak type 2 were diagnosed. The mean age in cases with beingn cysts was 46 ± 16.9 years (range - 34 to 58 years). Cysts demonstrated mean

Attenuation of 15 ± 1.4 HU. The mean cyst enhancement was 1.5 ± 3.5 HU during Corticomedulary phase and 2 ± 2.8 HU during nephrographic phase. The differences in mean enhasncement in corticomedullary phase and nephrographic phase was statistically insignificant.

Angiomylipoma

Table 31 – Age & size distribution and enhancement of angiomyolipoma

Angiomylipoma	Mean	Std. Deviation
AGE	39.25	5.058
SIZE	9.325	7.0159

Angiomylipoma	Mean HU	Std. Deviation
Unenhanced phase	-22.75	1.500
CMP	-19.50	3.109
NP	-16.50	3.697
Degree of enhancement in CMP	3.2500	2.62996
Degree of enhancement in NP	6.2500	4.11299

In my study 4 cases of angiomyolipoma were included. all cases of angiomyoliopa were present in females. the mean age was 39.25 ± 5 years (range 35 to 45 years). the mean size was 9.3 ± 7 cm (3 cm to 18 cm). the masses showed a mean attenuation of -22.75 ± 1.5 HU on unenhanced CT images. Cortical mean enhancement was -19± 3 HU during corticomeduallary phase and 16.5 ± 3.1 HU during nephrographic phase.

RENAL ABSCESS

Table 32 – Age & size distribution and enhancement of renal abscess

Renal abscess	Mean	Std. Deviation
AGE in years	47.86	13.422
SIZE in cm	3.986	1.8668

Renal abscess	Mean HU	Std. Deviation
Unenhanced phase	22.43	1.718
CMP	23.71	1.799
NP	24.14	1.464
Degree of enhancement in CMP	1.2857	.75593
Degree of enhancement in NP	1.7143	1.60357

In my study 7 cases of renal abscess were included since most of the lesions mimicked as a mass. out of 7 cases 3 were present in females and 4 in males. the mean age was 47.8 ± 13 years (range 26 to 63 years). the mean size was 3.9 ± 1.8 cm (2.1 cm to 7.2 cm). the masses showed a mean attenuation of 22.4 ± 1.7 HU on unenhanced CT images. Cortical mean enhancement was 23 ± 1.7 HU during corticomeduallary phase and 24.14 ± 1.4 HU during nephrographic phase. pain was most common complaint seen in all cases and fever in 6 out of 7 cases. The urine culture was positive in 6 out of 7 cases. other features such as focal or global enlargement of the kidney, perinephric stranding, thickening of Gerota fascia was seen in most cases. Based on these imaging findings the diagnosis of renal abscess was made. All the cases showed significant improvement after giving antibiotics $\pm$ percutaneous drainage.

TCC

A case of transitional cell carcinoma was included in my study. it was seen in a 70 year old male patient who presented with weight loss. it was a illdefined hypodense mass in pelvis extending to cortex and ureter. the attenuation on unenhanced CT images was 39 HU. on corticomedullary phase and nephrographic phase the attenuation was 82 and 76 HU respectievely. on biopsy mass was found to be TCC.

Oncocytoma

A single case of oncocytoma was included in my study. it was seen a 56 year old male patient. it presented as a well defined heterogenous mass on post contrast study. The attenuation of the mass on unenhanced CT images was 34 HU. On corticomedullary phase and nephrographic phase the attenuation was 78 and 89 HU respectievely. unlike RCC and TCC, oncocytoma showed gradual enhancement in nephrographic phase compared to corticomedullary phase. RCC and TCC showed wash out in nephrographic phase. a characteristic central scar was noted in mass which helped in radiological diagnosis of oncocytoma and this was proven on biopsy also.

Table 33 - Histopathological correlation

No of cases	CT diagnosis	Pathological diagnosis
11	RCC	RCC
2	BOSNIAK TYPE IV	RCC
1	RCC	RENAL METASTASIS – UNKNOWN PRIMARY
1	TRANSITIONAL CELL CARCINOMA	TRANSITIONAL CELL CARCINOMA
7	RENAL ABSCESS	RENAL ABSCESS
4	AML	AML
2	BOSNIAK TYPE II CYST	-
1	BOSNIAK TYPE III CYST	Lost in follow up
1	ONCOCYTOMA	ONCOCYTOMA

A total of 13 cases of renal cell carcinoma was included in my study. Two cases of RCC presented as a solid cystic mass with enhancing soft tissue components with no evidence of metastasis or renal vessel involvement. These masses were diagnosed as Bosniak type 4 cysts based on imaging findings. The lesions turned out to be renal cell carcinoma on biopsy. One mass was diagnosed as renal cell carcinoma based on enhancement >20 HU on corticomedullary and nephrographic phases. On biopsy the mass lesion was diagnosed as metastasis (adenocarcinoma) from an unknown primary.

In one patient two mass lesions were detected in lower pole of right kidney. It was a well defined cystic lesion with thick enhancing septations with no enhancing soft tissue component and it was classified as Bosniak type III cyst, however the patient refused biopsy and was lost in follow up and was excluded from the study.

Two cases of Bosniak type II cysts did not undergo any biopsy/surgical intervention because of its benign appearance on imaging.

REPRESENTATIVE CASES

Case 1 - renal cell carcinoma

UNENHANCED PHASE
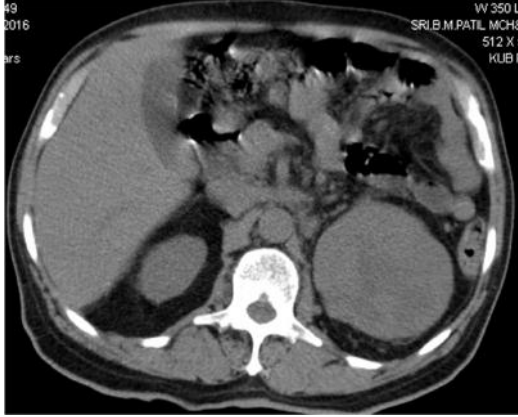
CORTICOMEDULLARY PHASE
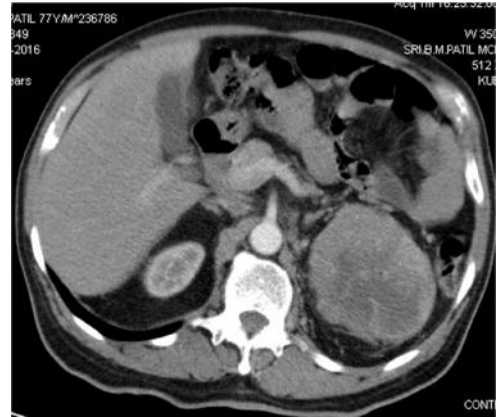
NEPHROGRAPHIC PHASE
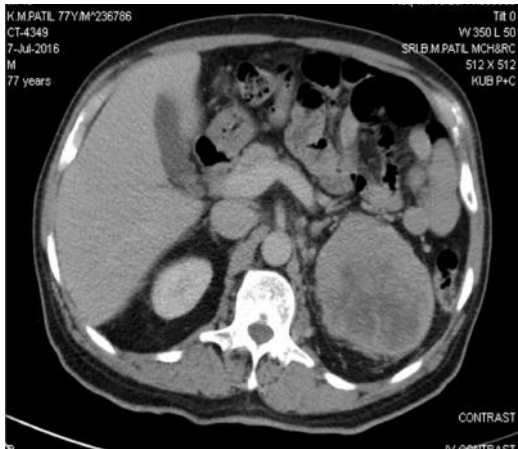
REFORMATTED CORONAL CT IMAGE

Case 2 - Transitional cell carcinoma.
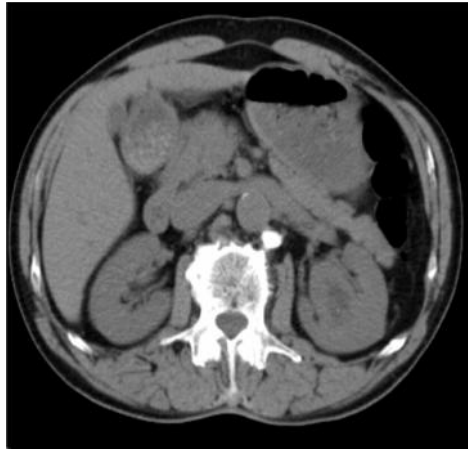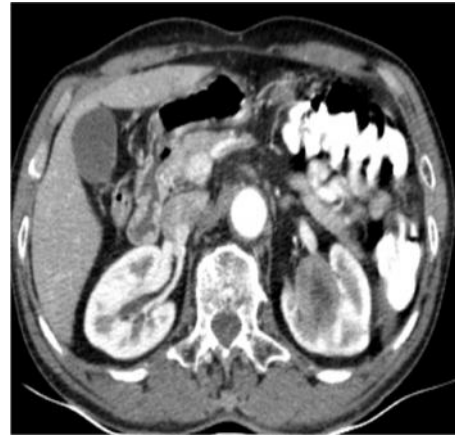
UNENHANCED PHASE

CORTICOMEDULLARY PHASE
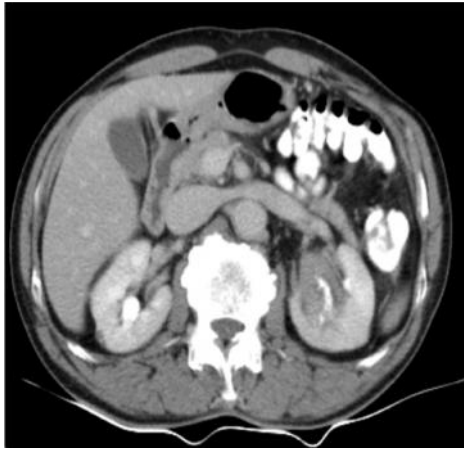
NEPHROGRAPHIC PHASE

REFORMATTED CORONAL CT IMAGE

TCC INVOLVING PROXIMAL URETER WITH DJ STENT.

Case 3 - RENAL METASTASIS (adenocarcinoma) from unknown primary
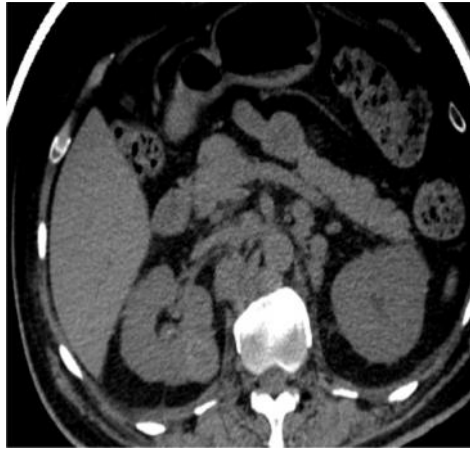
UNENHANCED PHASE

CORTICOMEDULLARY PHASE
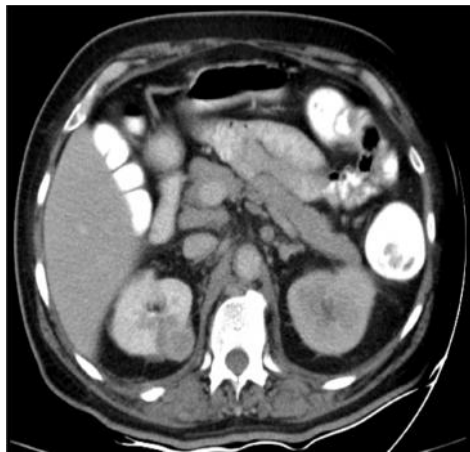
NEPHROGRAPHIC PHASE

PARAAORTIC AND PARACAVAL LYMPHADENOPATHY

Case 4 - ONCOCYTOMA

UNENHANCED PHASE

CORTICOMEDULLARY PHASE

NEPHROGRAPHIC PHASE

Case 5 - BOSNIAK TYPE IV CYST

UNENHANCED PHASE

CORTICOMEDULLARY PHASE

NEPHROGRAPHIC PHASE
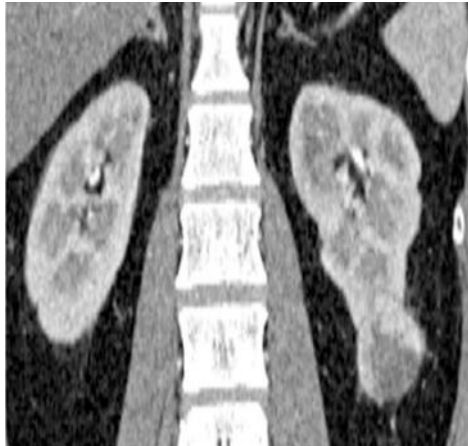
REFORMATTED CORONAL CT IMAGE

Case 6 - RENAL ABSCESS

UNENHANCED PHASE
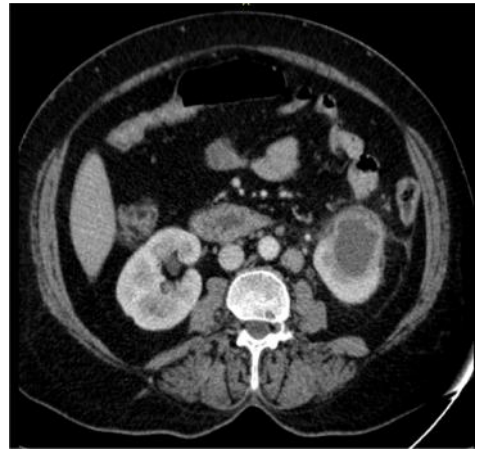
CORTICOMEDULLARY PHASE
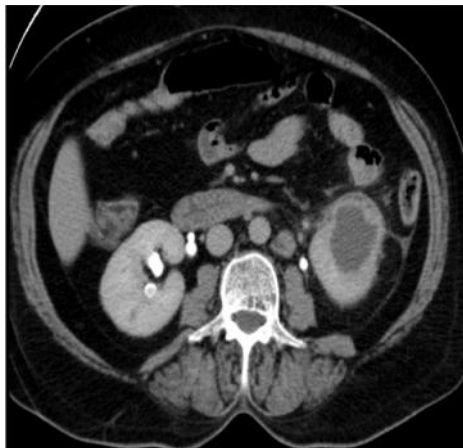
NEPHROGRAPHIC PHASE

DISCUSSION

MDCT continues to have a large impact on the diagnosis and characterization of renal masses. It is the only imaging modality which is required prior surgery. Advances in data acquisition and display provide tremendous capabilities in detection and management of renal masses.

To improve detection of renal masses, multiphasic CT study - precontrast and post contrast corticomedullary and nephrographic phases was used in the study because in a study by **Sheth et al.**[52] the images obtained only during the CMP phase has failed to identify many of the small renal masses that were easily seen on the NP. The post biopsy or surgical data were used as a reference standard.

Renal parenchymal tumours are heterogenous group consisting of benign to highly aggressive/malignant masses. The morphological features and the degree of enhancement vary significantly depending upon the type of tumour. The precise preoperative prediction of the histological type of lesion may be helpful not only for determining the appropriate treatment plan, such as the extent of the preoperative evaluation and surgery, but also in counselling the patient preoperatively. [71]

This is a cross sectional prospective study which included 30 consecutive cases of renal masses detected on MDCT.

The mean age of patients was 53 ± 12 years (range 26 to 82 years) which include 19 males and 11 females. The mean age of patients with malignant masses was 61.13 years and in patients with benign masses was 45.71 years.

Similarly in studies by **Cohan et al.** [7] who studied 33 patients with renal masses, age ranged from 37 to 82 years and mean age was 58.4 years. **Birnbaum et al.** [5] studied 30 patients whose age ranged from 41- 82 years and mean age was 62

years. **Welch et al.** [72] studied 73 patients whose age ranged from 14-80 years and mean age was 63.7 years.

In my series the incidence of RCC was seen at a younger age group. 7 out of 13 (53.8 %) cases of RCC were seen in the age group of 50 to 60 years with a mean age of 60.77 years (range 50 to 82 years). Similary in an Indian study by **Shalini Agnihotri et al.l** [49] 60.2 per cent of patients were below the age of 60 yr. However in a western study from **Surveillance Epidemiology and End Results (SEER)** [73] database, majority of RCC cases at presentation were between 60-69 or 70-79 yr of age and only 42 per cent of patients presented in < 60 yr of age.

In this series the distribution of renal masses were more in males (19 out of 30) than in females (11 out of 30) with a male to female sex ratio of 1.7: 1. The male to female sex ratio in patients with RCC was 2.2: 1 which included 9 males and 4 females. This is correlating with the studies conducted by **Birnbaum et al.** [5] and **Seuong Kwon Choi et al.** [71]. In their study, Male to female ratio was 2.2:1 and 2.9: 1 respectively. Similarly in a Indian study by **Shailender Singh et al.** [74] the male to female ratio was 2.9:1 in patients with RCC.

The most common presentation of renal masses in our setting was loin pain which was seen in 25 out of 30 cases (83 %), followed by weight loss in 10 cases (33 %), fever in 8 (26.7%), haematuria and lump in 6 (20%).

Where as in a study by **CM Shetty et al.** [75] on renal masses sixteen patients presented with hematuria, eleven patients with loin pain, four patients with Weight loss, one with fever and one patient was asymptomatic.

In our series the most common presentation in cases of renal cell carcinoma was pain in 12 cases (92 %), followed by weight loss in 8 (61.5%), haematuria in 4

(30.8%) and fever in 2 (15.4 %). Haemoglobin levels were decreased in 7 cases (46.2 %).

The classic triad of flank pain, hematuria, and flank mass was seen in 2 cases (15.3%) of renal cell carcinoma which was similar to a study by **Hatimota P et al.** [76] However in the same series by **Hatimota P et al.** [76] the most common presenting symptom was haematuria, followed by pain and weight loss.

Out of 30 cases, 14 cases were benign and 15 were malignant masses. In one patient two mass lesions were detected in lower pole of right kidney. It was a well-defined cystic lesion with thick enhancing septations and it was classified as Bosniak type III cyst, however the patient refused biopsy and was lost in follow up and was excluded from the study.

The benign lesions included 6 cases of renal abscess, 4 angiomylipoma, one oncocytoma and 2 cases of Bosniak type II cyst.

Among malignant masses, 13 cases were renal cell carcinoma. One transitional cell carcinoma of renal pelvis and one metastasis (adenocarcinoma) from unknown primary. RCC was the most common renal mass detected comprising of 43 % cases of renal masses.

Similary in studies by **Hatimota et al.** [76] RCC was the most common neoplasm. Renal cell carcinoma (n=38), followed by angiomyolipoma (n=5), renal metastases (n=3), oncocytoma (n=1), transitional cell carcinoma (n=1).

In a study by **Seung KWon et al.** [71] RCC was the most common neoplasm comprising of 80% cases. Followed by benign lesions in 20%.

There were 34 lesions in 30 patients. The size of the lesion ranged from 2-18 cm with mean size of 5.4 (± 3.5) cm.

Right kidney was involved in 13 (43.3 %), left in 16 (53.3 %) and bilaterally in one (3.3 %) cases. Two lesions were detected in each case of AML and renal abscess and three lesions in a case of renal abscess which was located bilaterally.

In a study by **Birnbaum et al.** [5], in his series the average size of the neoplasms was 4.3cm ± 1.8 (range,1.4-8.0 cm). The results of this study wass comparable to my study.

In a study by **CM Shetty et al.** [75] twenty three lesions were detected in twenty two patients. The size of the lesion ranged from 2.4-14 cm with mean size of 9.7 cm.

The study conducted by **Welch et al.** [72], size ranged from 1.5 to 19 cm (mean 7cm). The mean size of renal masses in present study is slightly lower that the study conducted by **CM Shetty et al.** [75] and **Welch et al.** [72]

In my study peripheral calcification was seen in 4 out of 14 cases among benign masses whereas malignant lesion did not show evidence of calcification. The calcification was noted in septae and walls of cystic masses.

Similarly in studies by **Philip J. Weyman et al.** [77] and **Israel GM et al.** [78] peripheral calcifications in septae and walls was noted in benign cystic lesions.

Comparison of enhancement of normal renal cortex.

The renal cortex demonstrated a mean attenuation of 32 ±3 HU on unenhanced CT images. Cortical mean enhancement was 122 ±15 HU during corticomeduallary phase and 137 ±9 HU during nephrographic phase. The degree of enhancemnt in corticomedullary and nephrographic phases were 90 ±16 and 105 ±10. There was a statically significant difference in enhnancement in corticomedullary and nephrographic phase (P <0.05).

Similar results were noted in a study by **Cm Shetty et al.** [75] . Renal cortex showed greater enhancement in the nephrographic phase compared with that in the corticomedullary phase.

In studies by **Cohan et al.** [7] and **Szolar et al.** [8] the mean cortical enhancement was greater in corticomedullary than in nephrographic phases.

The discrepancy in the cortical enhancement between present study and **Cohan et al.** [7] & **Szolar et al.** [8] studies are due to substantial differences in the rate of contrast injection and due to differences in the time of acquisition.

In present study, corticomedullary and nephrographic phase images are acquired between 30–40 seconds and 80–120 seconds after initiation of contrast injection respectively . 100 ml of contrast was injected at a rate of 3 ml/s in the present study. In **Cohan et al.** [7] study the time to acquire corticomedullary phase images was not specified. They acquired corticomedullary phase images anywhere between 40-70 seconds. Nephrographic phase images were acquired after mean time of 163 seconds after initiation of contrast injection. In **Szolar's** [8] study, corticomedullary phase images were acquired 50 seconds and 180 seconds after initiation of contrast injection respectively. So it is possible that the results in present study differed from results in **Cohan et al.** [7] and **Szolar et al.** [8] study.

Benign renal cysts.

Two radiologically benign cysts of Bosniak type II were diagnosed. The mean age in cases with beingn cysts was 46 ± 16.9 years (range - 34 to 58 years). Cysts demonstrated mean attenuation of 15 ± 1.4 HU. The mean cyst enhancement was 1.5 ± 3.5 HU during corticomedulary phase and 2 ± 2.8 HU during nephrographic phase. The differences in mean enhancement in corticomedullary and nephrographic phases was statistically insignificant.

These findings correlated with the study conducted by **Birnbaum et al. [5]** .

BENIGN VERSUS MALIGNANT LESIONS.

	BENIGN	MALIGNANT	P VALUE
NO OF CASES	14	15	
MEAN AGE	45.71 years ± 11.605	61.13 years ± 9.125	**0.001**
MALE TO FEMALE RATIO	1:1	2.7:1	0.196
SIZE in cm	5.6	5.56	0.981
SYMPTOMS PRESENT			
Pain	11	13	0.564
Hematuria	1	5	0.82
Weight loss	1	9	**0.003**
Lump	2	4	0.411
Fever	6	2	0.075
WELLDEFINED/ILLDEFINED	12/2	7/8	**0.027**
ATTENUATION			
Hypodense	13	13	
Isodense	1	1	
Hyperdense	0	1	
ENHANCEMENT PATTERN			**0.033**
Homogenous	7	2	
Heterogenous	7	13	
HOUNSFIELD UNITS (HU)			
Unenhanced phase	9.29 ± 21.514	34.87 ± 3.543	**0.001**
Corticomedullary phase	14.21 ± 26.762	96.53 ± 12.977	**0.001**
Nephrographic phase	16.14 ± 27.840	72.93 ± 10.194	**0.000**
Degree of enhancement in Corticomedullary phase	4.9286 ± 11.40489	61.6667 ± 15.29550	
Degree of enhancement in nephrographic phase	6.8571 ± 14.21190	38.0667 ± 10.85927	

In this series malignant renal mass was predominantly seen in older age group with higher male to female predominance. The malignant masses were predominantly ill-defined (8 0ut of 15 cases) whereas benign masses were predominantly well defined (12 out of 14 cases).

Similar results were seen in studies by **Cohan et al. [7], Birnbaum et al. [5], Welch et al. [72], Sun M et al. [73], Seuong Won Choi et al. [71].**

The malignant masses predominantly demonstrated heterogenous enhancement pattern in 13 out of 15 cases. A case of RCC measuring 2.1 cm displayed homogenous enhancement. A case of renal metastasis measuring about 2 cm from unknown primary also displayed homogenous enhancement

Similarly in a study by **Kim et al. [79]**, RCC above 3 cm in size predominantly demonstrated heterogenous enhancement. Homogenous enhancement was more commonly seen in RCC less than 3 cm in size.

In a study by **Russo P et al. [80]** The enhancement pattern of a tumor is generally affected by its size; the larger a tumor grows >5cm, the more frequently intratumoral necrosis or hemorrhage occurs.

In benign masses the homogenous and heterogenous enhancement pattern was equally distributed.

Furthermore in this study the attenuation value was useful in differentiating benign from malignant lesions. The mean attenuation value of malignant masses in unenhanced CT images was 34.8 HU whereas in benign masses was 9.2 HU. In corticomedullary phase the malignant masses showed rapid enhancement with a mean HU value of 96.53 ± 12.977 and a rapid decrease of in enhancement in following nephrographic phase with mean HU value of 72.93 ± 10.194. The differences in HU

between corticomedullary phase and nephrographic phase in cases of malignant and beingn masses was significant (p<.05).

In my study 13 cases of RCC had a mean attenuation value of 34.31 ± 2.2 HU on a unenhanced scan. All cases of RCC showed significant contrast enhancement in corticomedullary phase (99.54 ± 9.12) and washout in nephrographic phase (72 ± 10.8).

The ROC curve analysis showed that the cut off values with highest sensitivity and specificity for characterization of RCC from other masses was 71.5 HU in corticomedullary phase (sensitivity 100%, specificity 99.9%), 41.5 HU in nephrographic phase (sensitivity 100% , specificity 99.8 %).

The findings of prior studies are consistent with the results of this study. In a study by **Wahba Manal H et al.** [81], 39 RCC masses showed intense enhancement in the corticomedullary phase (mean 80.5 HU, ± 45.7), rapid decrease of enhancement in the following nephrographic phase (mean 70.6 HU, ± 25.4) denoting rapid wash out of contrast.

A study reported by **Kim et al.** [53] Showed that RCC had strong enhancement on biphasic ct, with a contrast enhancement of over 100 HU on the CMP, at 115±48 HU, compared with the level of enhancement on the excretory phase, at 62±25. **Jinzaki et al.** [55] compared the degree and pattern of contrast enhancement on the CMP and late NP with the findings of 40 renal neoplasms smaller than 3.5 cm. All clear cell types of RCC's exhibited a peak attenuation value on the CMP of more than 100 HU (165.0±45.8 HU), which was significantly higher than among the other renal tumors.

The strong enhancement in cases of RCC in corticomedullary phase was due to increased microvessel density (angiogenesis) [55]

The strong enhancement of conventional renal carcinoma is caused by its rich vascular network and alveolar architecture at histologic examination.[82,83]

CONCLUSION

- The study was primarily done to analyse attenuation values and enhancement pattern of renal masses during unenhanced, corticomedullary and nephrographic phases, for better detection and characterization of renal masses by multidetector computed tomography.

- In my study all renal masses were detected in both corticomedullary and nephrographic phases. For characterization of renal masses - the enhancement pattern, attenuation values in corticomedullary and nephrographic phases served as a valuable parameter in differentiating malignant from benign renal masses.

- No statistically significant differences ($p > 0.05$) in enhancement were noted for the radiologically benign cysts when the corticomedullary and nephrographic phases were compared.

- The malignant masses demonstrated greater enhancement in corticomedullary phase than in nephrographic phase (early enhancement - rapid washout)

- The normal renal cortex demonstrated greater enhancement in nephrographic phase than in corticomedullary phase.

- To conclude, MDCT protocol for evaluation of renal masses should include unenhanced, corticomedullary and nephrographic phases for better detection and characterization of renal masses.

LIMITATIONS

The threshold value we have reported is applicable only to patients with similar contrast injection protocols and scan delay times because the enhancement pattern could vary according to contrast injection variables and scan delay times. This study did not evaluate differences of each subtype of RCC because of small sample size.

SUMMARY

This was a cross sectional prospective study which included 30 consecutive cases of renal masses detected on MDCT. The study data was collected from July 2014 to June 2016 in the Department of Radio-diagnosis, Shri B.M. Patil Medical College Hospital and research center, Bijapur, Karnataka.

Attenuation values and enhancement pattern of renal masses during unenhanced, corticomedullary and nephrographic phases were analysed, for better detection and characterization of renal masses by multidetector computed tomography.

The mean age of patients was 53 ± 12 years (range 26 to 82 years) which include 19 males and 11 females. The mean age of patients with malignant masses was 61.13 years and in patients with benign masses was 45.71 years.

In this series the incidence of RCC was seen at a younger age group. 7 out of 13 (53.8 %) cases of RCC were seen in the age group of 50 to 60 years with a mean age of 60.77 years (range 50 to 82 years)

RCC was the most common renal mass detected comprising of 43 % cases of renal masses.

The malignant masses predominantly demonstrated heterogenous enhancement pattern. The mean attenuation value of malignant masses in unenhanced CT images was 34.8 HU. In corticomedullary phase the malignant masses showed rapid enhancement (mean HU value of 96.53 ± 12.977) followed by a rapid decrease of in enhancement in nephrographic phase (mean HU value of 72.93 ± 10.194). Similarly RCC showed greater enhancement in corticomedullary phase than in nephrographic phase. The ROC curve analysis showed that the cut off values with highest sensitivity and specificity for characterization of RCC from other masses was 71.5 HU in

corticomedullary phase (sensitivity 100%, specificity 99.9%), 41.5 HU in nephrographic phase (sensitivity 100%, specificity 99.8 %).

No statistically significant differences (p > 0.05) in enhancement were noted for the radiologically benign cysts when the corticomedullary and nephrographic phases were compared.

The normal renal cortex demonstrated greater enhancement in nephrographic phase (mean - 137 ± 9 HU) than in corticomedullary phase (mean -122± 15 HU).

To conclude, MDCT protocol for evaluation of renal masses should include unenhanced, corticomedullary and nephrographic phases for better detection and characterization of renal massses.

BIBLIOGRAPHY

1. Goldman LW. Principles of CT: multislice CT. J Nucl Med Technol. 2008;36(2):57-68-76.

2. Eble JN, Sauter G, Epstein JI SI. Pathology and genetics of tumours of the urinary system and male genital organs. IARC Press Lyon, France. 2004;

3. Bosniak MA. The current radiological approach to renal cysts. Radiology. 1986 Jan;158(1):1–10.

4. Brief History of CT. http://www.imaginis.com/ct-scan/brief-history-of-ct.

5. Birnbaum BA, Jacobs JE, Ramchandani P. Multiphasic renal CT: comparison of renal mass enhancement during the corticomedullary and nephrographic phases. Radiology. 1996 Sep;200(3):753–8.

6. Yuh BI, Cohan RH. Different phases of renal enhancement: role in detecting and characterizing renal masses during helical CT. AJR Am J Roentgenol. 1999 Sep;173(3):747–55.

7. Cohan RH, LS S, M K, JC B, IR F. Renal masses: assessment of corticomedullary-phase and nephrographic-phase CT scans. Radiology. 1995;96:445–51.

8. Szolar D, Kammerhuber F, Aliziebler S, Al E. Multiphasic helical CT of the kidney: increased conspicuity for detection and characterization of small (_3 cm)renal masses. Radiology. 1997;202:211–7.

9. Gillatt D, O'Reilly P. Haematuria analyzed: a prospective study. J R Soc Med. 1987;80:559–60.

10. Kass DA, Hricak H, Davidson AJ. Renal malignancies with normal excretory urograms. Am J Roentgenol [Internet]. 1983 Oct 1;141(4):731–4. Available from: http://dx.doi.org/10.2214/ajr.141.4.731

11. Parvey H, Thomas J, Bernardino M, PA B, Lewis E. Pitfalls in diagnosis of exophytic renal tumors. Urology. 1982;20:218–22.

12. Warshauer DM, McCarthy SM, Street L, Bookbinder MJ, Glickman MG, Richter J, et al. Detection of renal masses: sensitivities and specificities of excretory urography/linear tomography, US, and CT. Radiology. 1988;169(2):363–5.

13. Zagoria RJ. Imaging of small renal masses: a medical success story. AJR Am J Roentgenol. 2000;175(4):945–55.

14. Whalen JP. Caldwell Radiology of the Abdomen: Lecture. Impact of new imaging methods. AJR Am J Roentgenol. 1979 Oct;133(4):587–618.

15. Ng CS, Wood CG, Silverman PM, Tannir NM, Tamboli P, Sandler CM. Renal cell carcinoma: Diagnosis, staging, and surveillance. Am J Roentgenol. 2008;191(4):1220–32.

16. Bhatt S, MacLennan G, Dogra V. Renal pseudotumors. Am J Roentgenol. 2007;188(5):1380–7.

17. Segal AJ, Spitzer RM. Pseudo thick-walled renal cyst by CT. Am J Roentgenol [Internet]. 1979 May 1;132(5):827–8. Available from: http://dx.doi.org/10.2214/ajr.132.5.827

18. Curry NS, Schabel SI, Betsill WL. Small renal neoplasms: diagnostic imaging, pathologic features, and clinical course. Radiology [Internet]. 1986 Jan 1;158(1):113–7. Available from: http://dx.doi.org/10.1148/radiology.158.1.3940366

19. Bae KT, Heiken JP, Siegel CL, Bennett HF. Renal cysts: is attenuation artifactually increased on contrast-enhanced CT images? Radiology [Internet]. 2000;216(3):792–6. Available from:

http://www.ncbi.nlm.nih.gov/pubmed/10966713

20. Curry NS, Brock G, Metcalf JS, Sens MA. Hyperdense renal mass: unusual CT appearance of a benign renal cyst. Urol Radiol. 1982;4(1):33–5.

21. Fishman MC, Pollack HM, Arger PH, Banner MP. High protein content: another cause of CT hyperdense benign renal cyst. J Comput Assist Tomogr. 1983 Dec;7(6):1103–6.

22. Levine E, Grantham JJ. High-density renal cysts in autosomal dominant polycystic kidney disease demonstrated by CT. Radiology. 1985 Feb;154(2):477–82.

23. Dunnick NR, Korobkin M, Clark WM. CT demonstration of hyperdense renal carcinoma. J Comput Assist Tomogr. 1984 Oct;8(5):1023–4.

24. Hartman DS, Weatherby E 3rd, Laskin WB, Brody JM, Corse W, Baluch JD. Cystic renal cell carcinoma: CT findings simulating a benign hyperdense cyst. AJR Am J Roentgenol. 1992 Dec;159(6):1235–7.

25. Stunell H, McNeill G, Browne RFJ, Grainger R, Torreggiani WC. The imaging appearances of calyceal diverticula complicated by uroliathasis. Br J Radiol. 2010 Oct;83(994):888–94.

26. Gayer G, Apter S, Heyman Z, Morag B. Pyelocalyceal diverticula containing milk of calcium--CT diagnosis. Clin Radiol. 1998 May;53(5):369–71.

27. Elkin M. No Title. Radiol Urin Bost Little, Brown. 1980;962–3.

28. Hidalgo H, Dunnick NR, Rosenberg ER, Ram PC, Korobkin M. Parapelvic cysts: Appearance on CT and sonography. Am J Roentgenol. 1982;138(4):667–71.

29. Chan JCM, Kodroff MB. Hypertension and Hematuria Secondary to Parapelvic Cyst. Pediatrics [Internet]. 1980 Apr 1;65(4):821 LP-823. Available from:

http://pediatrics.aappublications.org/content/65/4/821.abstract

30. Amin MB, Crotty TB, Tickoo SK, Farrow GM. Renal Oncocytoma: A Reappraisal of Morphologic Features with Clinicopathologic Findings in 80 Cases. Am J Surg Pathol [Internet]. 1997;21(1). Available from: http://journals.lww.com/ajsp/Fulltext/1997/01000/Renal__Oncocytoma__A_Re appraisal_of_Morphologic.1.aspx

31. Chao DH, Zisman A, Pantuck AJ, Freedland SJ, Said JW, Belldegrun AS. Changing concepts in the management of renal oncocytoma. Urology [Internet]. 2016 Oct 19;59(5):635–42. Available from: http://dx.doi.org/10.1016/S0090-4295(01)01630-2

32. Kim JI, Cho JY, Moon KC, Lee HJ, Kim SH. Segmental enhancement inversion at biphasic multidetector CT: characteristic finding of small renal oncocytoma. Radiology. 2009;252(2):441–8.

33. Schieda N, McInnes MDF, Cao L. Diagnostic accuracy of segmental enhancement inversion for diagnosis of renal oncocytoma at biphasic contrast enhanced CT: systematic review. Eur Radiol [Internet]. 2014;24(6):1421–9. Available from: http://dx.doi.org/10.1007/s00330-014-3147-4

34. Gakis G, Kramer U, Schilling D, Kruck S, Stenzl A, Schlemmer H-P. Small renal Oncocytomas: Differentiation with multiphase CT. Eur J Radiol [Internet]. 2016 Oct 19;80(2):274–8. Available from: http://dx.doi.org/10.1016/j.ejrad.2010.06.049

35. Bird VG, Kanagarajah P, Morillo G, Caruso DJ, Ayyathurai R, Leveillee R, et al. Differentiation of oncocytoma and renal cell carcinoma in small renal masses (<4 cm): the role of 4-phase computerized tomography. World J Urol [Internet]. 2011;29(6):787–92. Available from:

http://dx.doi.org/10.1007/s00345-010-0586-7

36. Young JR, Margolis D, Sauk S, Pantuck AJ, Sayre J, Raman SS. Clear Cell Renal Cell Carcinoma: Discrimination from Other Renal Cell Carcinoma Subtypes and Oncocytoma at Multiphasic Multidetector CT. Radiology [Internet]. 2013 May 1;267(2):444–53. Available from: http://dx.doi.org/10.1148/radiol.13112617

37. Pierorazio PM, Hyams ES, Tsai S, Feng Z, Trock BJ, Mullins JK, et al. Multiphasic Enhancement Patterns of Small Renal Masses (≤4 cm) on Preoperative Computed Tomography: Utility for Distinguishing Subtypes of Renal Cell Carcinoma, Angiomyolipoma, and Oncocytoma. Urology [Internet]. 2016 Oct 19;81(6):1265–72. Available from: http://dx.doi.org/10.1016/j.urology.2012.12.049

38. Zhang J, Lefkowitz RA, Ishill NM, Wang L, Moskowitz CS, Russo P, et al. Solid Renal Cortical Tumors: Differentiation with CT. Radiology [Internet]. 2007 Aug 1;244(2):494–504. Available from: http://dx.doi.org/10.1148/radiol.2442060927

39. Eble JN. Angiomyolipoma of kidney. Semin Diagn Pathol. 1998 Feb;15(1):21–40.

40. Casper KA, Donnelly LF, Chen B, Bissler JJ. Tuberous sclerosis complex: renal imaging findings. Radiology. 2002 Nov;225(2):451–6.

41. Kim JK, Park S-Y, Shon J-H, Cho K-S. Angiomyolipoma with minimal fat: differentiation from renal cell carcinoma at biphasic helical CT. Radiology. 2004;230(3):677–84.

42. Davenport MS, Neville AM, Ellis JH, Cohan RH, Chaudhry HS, Leder RA. Diagnosis of renal angiomyolipoma with hounsfield unit thresholds: effect of

size of region of interest and nephrographic phase imaging. Radiology. 2011 Jul;260(1):158–65.

43. Yamakado K, Tanaka N, Nakagawa T, Kobayashi S, Yanagawa M, Takeda K. Renal angiomyolipoma: relationships between tumor size, aneurysm formation, and rupture. Radiology. 2002;225(1):78–82.

44. Jemal A, Siegel R, Ward E, Murray T, Xu J, Thun MJ. Cancer statistics, 2007. CA Cancer J Clin. 2007;57(1):43–66.

45. National Cancer Data Base (NCDB). http://www.facs.org/cancer/ncdb/index.html. September 30,. 2015.

46. Choyke Pl, Amis ES, Bigongiari LR et al. ACR appropriateness criteria: renal cell carcinoma staging. American College of Radiology Website: www.acr.org. 1998.

47. Federle MP, Jeffrey RB WP et-al. Diagnostic Imaging: Abdomen, Published by Amirsys®. Lippincott Williams & Wilkins. 2009.

48. Doherty JG, Rüfer a, Bartholomew P, Beaumont DM. The presentation, treatment and outcome of renal cell carcinoma in old age. Age Ageing [Internet]. 1999;28(4):359–62. Available from: http://www.ncbi.nlm.nih.gov/pubmed/14527912

49. Agnihotri S, Kumar J, Jain M, Kapoor R. Renal cell carcinoma in India demonstrates early age of onset & a late stage of presentation. Indian J Med Res [Internet]. 2014;7(November):624–9. Available from: http://www.ncbi.nlm.nih.gov/pmc/articles/PMC4311315/

50. Patard J-J, Rodriguez A, Rioux-Leclercq N, Guille F, Lobel B. Prognostic significance of the mode of detection in renal tumours. BJU Int. 2002 Sep;90(4):358–63.

51. Jain P, Surdas R, Aga P, Jain M, Kapoor R, Srivastava A. Renal cell carcinoma：Impact of mode of detection on its pathological characteristics. Indian J Urol. 2009;25(December):479–82.

52. Sheth S, Scatarige JC, Horton KM, Corl FM, Fishman EK. Current concepts in the diagnosis and management of renal cell carcinoma: role of multidetector ct and three-dimensional CT. Radiographics. 2001;21 Spec No:S237–54.

53. Kim JK, Kim TK, Kim CS, Kim K, Cho K. Differentiation of Subtypes of Renal Cell Carcinoma on Helical CT Scans. AJR. 2002;(June):1499–506.

54. Prasad SR, Humphrey P a, Catena JR, Narra VR, Srigley JR, Cortez AD, et al. Common and uncommon histologic subtypes of renal cell carcinoma: imaging spectrum with pathologic correlation. Radiographics. 2006;26:1795-1806-1810.

55. Jinzaki M, Tanimoto A, Mukai M, Ikeda E, Kobayashi S, Yuasa Y, et al. Double-phase helical CT of small renal parenchymal neoplasms: correlation with pathologic findings and tumor angiogenesis. J Comput Assist Tomogr. 2000;24(6):835–42.

56. HU Y, Lu G-M, Li K, Zhang L-J, Zhu H. Collecting duct carcinoma of the kidney: Imaging observations of a rare tumor. Oncol Lett. 2014 Feb;7(2):519–24.

57. Moch H. [The WHO/ISUP grading system for renal carcinoma]. Pathologe. 2016 Jul;37(4):355–60.

58. Edge SB, Byrd DR, Compton CC, Fritz AG, Greene FL, Trotti A et al. AJCC Cancer Staging Manual. 7th ed. New York, NY: Springer-Verlag. 2010.

59. Nese N, Paner GP, Mallin K, Ritchey J, Stewart A, Amin MB. Renal cell carcinoma: assessment of key pathologic prognostic parameters and patient

characteristics in 47,909 cases using the National Cancer Data Base. Ann Diagn Pathol. 2009 Feb;13(1):1–8.

60.   Klatte T, Patard J-J, de Martino M, Bensalah K, Verhoest G, de la Taille A, et al. Tumor size does not predict risk of metastatic disease or prognosis of small renal cell carcinomas. J Urol. 2008 May;179(5):1719–26.

61.   Seute T, Leffers P, ten Velde GPM, Twijnstra A. Detection of brain metastases from small cell lung cancer: consequences of changing imaging techniques (CT versus MRI). Cancer. 2008 Apr;112(8):1827–34.

62.   Fuccio C, Ceci F, Castellucci P, Spinapolice EG, Palumbo R, D'Ambrosio D, et al. Restaging clear cell renal carcinoma with 18F-FDG PET/CT. Clin Nucl Med. 2014 Jun;39(6):e320-4.

63.   Prando A, Prando P, Prando D. Urothelial cancer of the renal pelvicaliceal system: unusual imaging manifestations. Radiographics [Internet]. 2010;30(6):1553–66. Available from: http://www.ncbi.nlm.nih.gov/pubmed/21071375

64.   Kirkali Z, Tuzel E. Transitional cell carcinoma of the ureter and renal pelvis. Crit Rev Oncol Hematol. 2003 Aug;47(2):155–69.

65.   Nocks BN, Heney NM, Daly JJ, Perrone TA, Griffin PP, Prout GRJ. Transitional cell carcinoma of renal pelvis. Urology. 1982 May;19(5):472–7.

66.   Wong-You-Cheong JJ, Wagner BJ, Davis CJJ. Transitional cell carcinoma of the urinary tract: radiologic-pathologic correlation. Radiographics. 1998;18(1):123–42; quiz 148.

67.   Baron RL, McClennan BL, Lee JK, Lawson TL. Computed tomography of transitional-cell carcinoma of the renal pelvis and ureter. Radiology. 1982 Jul;144(1):125–30.

68. Vikram R, Sandler CM, Ng CS. Imaging and staging of transitional cell carcinoma: part 2, upper urinary tract. AJR Am J Roentgenol. 2009 Jun;192(6):1488–93.

69. Balfe DM, McClennan BL, Stanley RJ, Weyman PJ, Sagel SS. Evaluation of renal masses considered indeterminate on computed tomography. Radiology. 1982 Feb;142(2):421–8.

70. Morehouse HT, Hoffman C. Imaging in Inflammatory Disease of the Kidney. AJR Am J Roentgenol. 1984;143:135–41.

71. Choi S, Jeon SH, Chang S. Urological Oncology Characterization of Small Renal Masses Less than 4 cm with Quadriphasic Multidetector Helical Computed Tomography : Differentiation of Benign and Malignant Lesions. Korean J Urol. 2012;53:159–64.

72. Welch TJ, LeRoy AJ. Helical and electron beam CT scanning in the evaluation of renal vein involvement in patients with renal cell carcinoma. J Comput Assist Tomogr. 1997;21(3):467–71.

73. Sun M, Abdollah F, Bianchi M, Trinh Q-D, Jeldres C, Tian Z, et al. A stage-for-stage and grade-for-grade analysis of cancer-specific mortality rates in renal cell carcinoma according to age: a competing-risks regression analysis. Eur Urol. 2011 Dec;60(6):1152–9.

74. Shailender Singh N SH. No Study to find the efficiency of multi-detector computed tomography in evaluation of renal massesTitle. Int J Recent Trends Sci Technol. 2014;12(1):4–7.

75. Shetty C, Lakhar B, Devi B, Lakshmi B. Dual-phase helical CT of kidney : Comparison of corticomedullary and nephrographic phases in detection and characterization of renal masses. Indian J Radiol Imaging [Internet]. 2004 Jul

1;14(3):285–90. Available from: http://www.ijri.org/article.asp?issn=0971-3026

76. Hatimota P, Vashist S, Aggarwal K, Kapoor A, Gupta N. Spectrum of US and CT findings in renal neoplasms with pathologic correlation. Indian J Radiol Imaging [Internet]. 2005 Jan 1;15(1):117–25. Available from: http://www.ijri.org/article.asp?issn=0971-3026

77. Weyman PJ, McClennan BL, Lee JK, Stanley RJ. CT of calcified renal masses. AJR Am J Roentgenol. 1982 Jun;138(6):1095–9.

78. Israel GM, Bosniak MA. Calcification in cystic renal masses: is it important in diagnosis? Radiology. 2003 Jan;226(1):47–52.

79. Park H, Park JY, Kim DY, Ahn SH, Chon CY, Han KH, et al. Characterization of focal liver masses using acoustic radiation force impulse elastography. World J Gastroenterol. 2013;19(2):219–26.

80. Russo P. Renal cell carcinoma: presentation, staging, and surgical treatment. Semin Oncol. 2000 Apr;27(2):160–76.

81. Wahba MH, Kassem TW, Mahmoud AAS. Role of multiphasic multi-detector computed tomography (MDCT) in the diagnosis and staging of solid neoplastic renal masses. Egypt J Radiol Nucl Med [Internet]. 2015;46(1):215–24. Available from: http://dx.doi.org/10.1016/j.ejrnm.2014.09.004

82. Reuter VE, Presti JCJ. Contemporary approach to the classification of renal epithelial tumors. Semin Oncol. 2000 Apr;27(2):124–37.

83. Fujimoto H, Wakao F, Moriyama N, Tobisu K, Sakamoto M, Kakizoe T. Alveolar architecture of clear cell renal carcinomas (< or = 5.0 cm) show high attenuation on dynamic CT scanning. Jpn J Clin Oncol. 1999 Apr;29(4):198–203.

ANNEXURES

ETHICAL CLEARANCE

B.L.D.E. UNIVERSITY'S
SHRI.B.M.PATIL MEDICAL COLLEGE, BIJAPUR-586 103
INSTITUTIONAL ETHICAL COMMITTEE
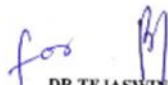
INSTITUTIONAL ETHICAL CLEARANCE CERTIFICATE

The Ethical Committee of this college met on 22-11-2014 at 3-30pm to scrutinize the Synopsis of Postgraduate Students of this college from Ethical Clearance point of view. After scrutiny the following original/corrected & revised version synopsis of the Thesis has been accorded Ethical Clearance.

Title "Detection and characterisation of renal Masses by Multidefector computed tomography"
——×——×——×——

Name of P.G. student _Dr. Nandish. H.R._
Dept of Radiology.

Name of Guide/Co-investigator Dr _B.R. Dhamanagaonkar,_
Professor of Radiology.

DR.TEJASWINI. VALLABHA
CHAIRMAN
INSTITUTIONAL ETHICAL COMMITTEE
BLDEU'S, SHRI.B.M.PATIL
MEDICAL COLLEGE, BIJAPUR.

Following documents were placed before E.C. for Scrutinization
1) Copy of Synopsis/Research project.
2) Copy of informed consent form
3) Any other relevant documents.

CONSENT FORM

B.L.D.E.U'S SHRI B.M.PATIL MEDICAL COLLEGE HOSPITAL AND RESEARCH CENTER, BIJAPUR-586103

RESEARCH INFORMED CONSENT FORM

TITLE OF THE PROJECT: **"DETECTION AND CHARACTERISATION OF RENAL MASSES BY MULTIDETECTOR COMPUTED TOMOGRAPHY."**

PRINCIPAL INVESTIGATOR: **Dr. NANDISH. H. R.** _{MBBS}

POST GRADUATE

DEPARTMENT OF RADIO DIAGNOSIS

Email: dr.nandish.hr@gmail.com.

P.G.GUIDE: **Dr. B R DHAMANGOANKAR** _{M.D.,D.M. R.D.}

PROFESSOR

DEPARTMENT OF RADIO DIAGNOSIS

PURPOSE OF RESEARCH:

I have been informed that this study is **"DETECTION AND CHARACTERISATION OF RENAL MASSES BY MULTIDETECTOR COMPUTED TOMOGRAPHY."**

I have been explained about the reason for doing this study and selecting me/my ward as a subject for this study. I have also been given free choice for either being included or not in the study.

PROCEDURE:

I/my ward have been explained that, I/my ward will be subjected to Contrast enhanced CT KUB/ABDOMEN for evaluation of the kidneys.

RISKS AND DISCOMFORTS:

I/my ward understand that necessary measures will be taken to reduce these complications as and when they arise.

BENEFITS:

I/my ward understand that my participation in this study will help to evaluate in the detection and characterization of renal masses.

CONFIDENTIALITY:

I/my ward understand that medical information produced by this study will become a part of this Hospital records and will be subjected to the confidentiality and privacy regulation of this hospital. Information of a sensitive, personal nature will not be a part of the medical records, but will be stored in the investigator's research file and identified only by a code number. The code key connecting name to numbers will be kept in a separate secure location.

If the data are used for publication in the medical literature or for teaching purpose, no names will be used and other identifiers such as photographs and audio or video tapes will be used only with my special written permission. I understand that I may see the photograph and videotapes and hear audiotapes before giving this permission.

REQUEST FOR MORE INFORMATION:

I understand that I may ask more questions about the study at any time. Dr.Nandish H. R. is available to answer my questions or concerns. I/my ward understand that I will be informed of any significant new findings discovered during the course of this study, which might influence my continued participation.

If during this study, or later, I wish to discuss my participation in or concerns regarding this study with a person not directly involved, I am aware that the social

worker of the hospital is available to talk with me and that a copy of this consent form will be given to me for careful reading.

REFUSAL OR WITHDRAWAL OF PARTICIPATION:

I/my ward understand that my participation is voluntary and I may refuse to participate or may withdraw consent and discontinue participation in the study at any time without prejudice to my present or future care at this hospital.

I/my ward also understand that Dr.Nandish H. R. will terminate my participation in this study at any time after he has explained the reasons for doing so and has helped arrange for my continued care by my own physician or therapist, if this is appropriate.

INJURY STATEMENT:

I understand that in the unlikely event of injury to me/my ward, resulting directly to my participation in this study, if such injury were reported promptly, then medical treatment would be available to me, but no further compensation will be provided.

I understand that by my agreement to participate in this study, I am not waiving any of my legal rights.

I have explained to _____ the purpose of this research, the procedures required and the possible risks and benefits, to the best of my ability in patient's own language.

Date: **Dr. B R Dhamangoankar**   **Dr.Nandish H. R.**

                              (Guide)   (Investigator)

PROFORME

1. PERSONAL DATA

NAME		AGE/SEX		IP/OP NO	
USG NO		UNIT	URIO/2	CASE NO	
DOE		DOA		DOD	
OCCUPATION		PLACE			

2. PRESENT HISTORY

Symptoms		Duration
Pain abdomen	Yes/no	
Hematuria	Yes/no	
Increased freq of micutrration	Yes/no	
Puffiness of face	Yes/no	
Swelling of limb	Yes/no	
Burring of limb	Yes/no	
Fever and chills	Yes/no	
Hypertension	Yes/no	
Others	Yes/no	

3. PAST HISTORY:

Rebnal calulus	Yes/no
Retention of urine	Yes/no
H/O HTN/DM/TB/SLE	Yes/no
Dialysis	Yes/no
Operation	Yes/no
Drug intake	Yes/no

4. Family history

   H/o renal calculus

   H/o renal malignancy

   H/o DM/HTN/TB

5. CLINICAL EXAMINATION

GENERAL

Pallor	Yes/no	Edema	Yes/no	Nails	
Cyanosis	yes/no	Ictrus	Yes/ no	Lymphadenopathy	Yes/no

Pulse:

Bp:

Temperature

Respiratory rate:

6. SYSTEMIC EXAMINATION:

Oer abdomen

a) Mass per abdomen

b) Tenderness

c) Others

RS:

CVS:

CNS:

7. UROGENTIAL SYSTEM

Renal angle tenderness – yes/no

Renal	Right	Let
Size		
Shape		
Surface		
Margin		
Consistency		
Mobility		
Tenderness		
Ballotment		
Percussion		
Auscultation		

Bladder

Focal lesion

Bladder calculus

Others

8. Provisional diagnosis

   1.

   2.

9. Investigations

   1. Blood-

Hb	%	Blood urea	Mg/dl	Sr. Creatinine	Mg/ dl

   2. Urine routine

Albumin	Yes/no	Sugar	Yes/no	Microscopy	

10. Radiological investigation

   A. KUB Radiogram:

   B. IVP:

   C. SONOGRAPHY

11. CT EVALUATION

I. Morphology of kidneys

	Right	Left
Position		
Size bipolar length		
Transverse diameter		
AP diameter		
Shape		

II. Secondary changes :

Renal calculi	Yes/no
Sol: size	Yes/no
Shape	
Region of origin	
Homogenous/ hetergenous	
Effects on kidney	
Calcification	Present/absent
Necrosis	Present/absent
UE HU	
CMP HU	
NP HU	
RV involvement	Present/absent
IVC invasion	Present/absent
RT atrium invasion	Present/absent

Lymph nodes	Present/absent
Adrenals	Present/absent
Long bones	Present/absent

III.   Renal sinuses

Calyces		
Pelvis		
Obstruction	GR/I/II/III	GR I/II/III
Ureters		
Bladder		
Associated findings		

RADIOLOGICAL DIAGNOSIS:

12. OTHER INVESTIGATIONS

    1. MRI

    2. Angiography

    3. Image Guided Biopsy

13. PATHLOGICAL DIAGNOSIS/ PER OPERATIVE DAIGNOSIS

FINAL DIAGNOSIS:

RESULTS:

SUMMARY:

KEY TO MASTER CHART

RFT **:** Renal function test

LFT **:** Liver function test

HPR **:** Histopathological report

NP **:** Nephrographic phase of normal

CMP **:** Corticomedullary Phase

CMP_CORTEX_NORMAL: Enhancement of renal cortex in corticomedullary phase.

CMP MEDULLA Normal : Enhancement of renal medulla in corticomedullary phase.

NP_Normal cortex : Enhancement of renal cortex in nephrographic phase.

Unenhanced phase RM : Attenuation of renal mass in unenhanced CT image.

CMP_RM : Enhancement of renal mass in corticomedullary phase.

NP_RM : Enhancement of renal mass in nephrographic phase.

ENH CMP RM : Degree of enhancement of renal mass in corticomedullary phase.

ENH NP RM : Degree of enhancement of renal mass in nephrographic phase.

Normal_cm_enh : Degree of enhancement of normal renal cortex in corticomedullary phase.

Normal_np_enh : Degree of enhancement of normal renal cortex in nephrographic phase.

MASTER CHART

serial no	age	sex	PAIN	LUMP	HEMATURIA	FEVER	WEIGHTLOSS	HB	OTHERSYMPTOMS	RFT	LFT	URINERBC	URINECULTURE	KIDNEY_SIDE	NO_of_LESIONS	LOCATION	CORTEX_MEDULLA	URETER	SIZE
1	70	MALE	ABSENT	ABSENT	PRESENT	ABSENT	ABSENT	NORMAL	2	NORMAL	NORMAL	PRESENT	negative	LEFT	1	interpolar	CM AND URETER	INVOLVED	3.5
2	56	MALE	PRESENT	ABSENT	ABSENT	ABSENT	ABSENT	NORMAL	2	NORMAL	NORMAL	ABSENT	negative	RIGHT	1	upper pole	CORTEX	NOT INVOLVED	2.1
3	77	MALE	PRESENT	PRESENT	PRESENT	ABSENT	PRESENT	DEARRANGED	2	NORMAL	NORMAL	PRESENT	negative	LEFT	1	upper pole	CORTEX	NOT INVOLVED	8.1
4	52	FEMALE	PRESENT	ABSENT	ABSENT	PRESENT	PRESENT	NORMAL	2	NORMAL	NORMAL	PRESENT	positive	RIGHT	2	UPPER AND LOWER	CORTEX	NOT INVOLVED	3
5	50	MALE	PRESENT	PRESENT	PRESENT	ABSENT	PRESENT	DEARRANGED	2	NORMAL	NORMAL	PRESENT	negative	RIGHT	1	UPPER AND MID	CORTEX	NOT INVOLVED	5.5
6	62	FEMALE	PRESENT	PRESENT	ABSENT	ABSENT	PRESENT	DEARRANGED	2	DEARRANGED	DEARRANGED	ABSENT	negative	RIGHT	1	UPPER AND MID	CORTEX	NOT INVOLVED	4.8
7	82	MALE	PRESENT	ABSENT	ABSENT	ABSENT	PRESENT	DEARRANGED	2	NORMAL	NORMAL	ABSENT	negative	LEFT	1	MID AND LOWER	CORTEX	NOT INVOLVED	7
8	57	MALE	ABSENT	ABSENT	ABSENT	PRESENT	ABSENT	NORMAL	2	NORMAL	NORMAL	ABSENT	negative	RIGHT	1	whole kidney	CORTEX AND MEDULLA	NOT INVOLVED	7.5
9	52	MALE	PRESENT	PRESENT	ABSENT	ABSENT	ABSENT	NORMAL	2	NORMAL	NORMAL	ABSENT	negative	LEFT	1	UPPER AND LOWER	CORTEX AND MEDULLA	NOT INVOLVED	13
10	45	FEMALE	PRESENT	ABSENT	ABSENT	ABSENT	ABSENT	NORMAL	2	NORMAL	NORMAL	ABSENT	negative	LEFT	1	upper pole	CORTEX	NOT INVOLVED	12
11	35	FEMALE	PRESENT	PRESENT	ABSENT	ABSENT	ABSENT	NORMAL	2	NORMAL	NORMAL	ABSENT	negative	RIGHT	1	whole kidney	CORTEX	NOT INVOLVED	18
12	42	FEMALE	ABSENT	ABSENT	ABSENT	ABSENT	ABSENT	NORMAL	2	NORMAL	NORMAL	ABSENT	negative	LEFT	1	upper pole	CORTEX	NOT INVOLVED	3
13	52	FEMALE	PRESENT	ABSENT	ABSENT	PRESENT	ABSENT	NORMAL	2	NORMAL	NORMAL	PRESENT	positive	BILATERAL	3	whole kidney	CORTEX	NOT INVOLVED	3
14	58	MALE	PRESENT	ABSENT	ABSENT	ABSENT	ABSENT	NORMAL	2	NORMAL	NORMAL	ABSENT	negative	LEFT	1	interpolar	CORTEX	NOT INVOLVED	3.3
15	34	MALE	ABSENT	ABSENT	ABSENT	ABSENT	ABSENT	NORMAL	2	NORMAL	NORMAL	ABSENT	negative	LEFT	1	UPPER AND MID	CORTEX	NOT INVOLVED	3.6
16	63	MALE	PRESENT	ABSENT	ABSENT	PRESENT	ABSENT	NORMAL	2	NORMAL	NORMAL	ABSENT	positive	LEFT	1	lower pole	CORTEX	NOT INVOLVED	2.1
17	60	MALE	PRESENT	ABSENT	ABSENT	PRESENT	ABSENT	NORMAL	2	NORMAL	NORMAL	PRESENT	positive	RIGHT	1	upper pole	CORTEX	NOT INVOLVED	3.5
18	48	FEMALE	PRESENT	ABSENT	ABSENT	PRESENT	ABSENT	NORMAL	2	NORMAL	NORMAL	ABSENT	positive	LEFT	1	lower pole	CORTEX	NOT INVOLVED	3.1
19	26	MALE	PRESENT	ABSENT	ABSENT	PRESENT	ABSENT	NORMAL	2	NORMAL	NORMAL	ABSENT	positive	LEFT	1	MID AND LOWER	CORTEX	NOT INVOLVED	6
20	35	FEMALE	ABSENT	ABSENT	ABSENT	ABSENT	ABSENT	NORMAL	2	NORMAL	NORMAL	ABSENT	negative	RIGHT	1	upper pole	CORTEX	NOT INVOLVED	4.3
21	57	MALE	PRESENT	ABSENT	ABSENT	ABSENT	ABSENT	NORMAL	2	NORMAL	NORMAL	ABSENT	negative	RIGHT	1	interpolar	CORTEX	NOT INVOLVED	4.4
22	55	FEMALE	PRESENT	ABSENT	ABSENT	ABSENT	PRESENT	NORMAL	2	NORMAL	NORMAL	ABSENT	negative	LEFT	1	upper pole	CORTEX	NOT INVOLVED	3.5
23	62	MALE	PRESENT	ABSENT	PRESENT	ABSENT	PRESENT	NORMAL	2	NORMAL	NORMAL	ABSENT	negative	RIGHT	1	UPPER AND MID	CORTEX	NOT INVOLVED	5.1
24	66	FEMALE	PRESENT	ABSENT	PRESENT	ABSENT	PRESENT	DEARRANGED	2	NORMAL	NORMAL	PRESENT	negative	LEFT	1	MID AND LOWER	CORTEX	NOT INVOLVED	6
25	34	MALE	PRESENT	ABSENT	PRESENT	ABSENT	ABSENT	NORMAL	2	NORMAL	NORMAL	PRESENT	negative	LEFT	1	MID AND LOWER	CORTEX	NOT INVOLVED	7.2
26	45	MALE	PRESENT	ABSENT	ABSENT	ABSENT	ABSENT	NORMAL	2	NORMAL	NORMAL	ABSENT	negative	RIGHT	2	lower pole	CORTEX	NOT INVOLVED	2
27	57	MALE	PRESENT	ABSENT	ABSENT	ABSENT	PRESENT	NORMAL	2	NORMAL	NORMAL	ABSENT	22	RIGHT	1	upper pole	CORTEX	NOT INVOLVED	2
28	54	MALE	PRESENT	ABSENT	ABSENT	ABSENT	ABSENT	NORMAL	2	NORMAL	NORMAL	ABSENT	negative	LEFT	1	lower pole	CORTEX	NOT INVOLVED	4.3
29	60	FEMALE	PRESENT	ABSENT	ABSENT	PRESENT	PRESENT	DEARRANGED	2	NORMAL	NORMAL	ABSENT	negative	RIGHT	1	lower pole	CORTEX	NOT INVOLVED	6.7
30	56	MALE	PRESENT	PRESENT	ABSENT	ABSENT	ABSENT	NORMAL	2	NORMAL	NORMAL	ABSENT	negative	LEFT	1	interpolar	CORTEX	NOT INVOLVED	6.3

MASTER CHART

HOMO_HETERO_MASS	DENSITY	WELL_ILL_DEFINED	CALCIFICATION	RENAL VEIN_IVC	HYDRONEPHROSIS	Imaging diagnosis	HPR	Uennhanced normal Parenchyma	CMP CORTEX NORMAL	CMP MEDULLA Normal cortex	NP_Normal cortex	Unenhanced phase_RM	CMP_RM	NP_RM	METASTASIS	ENH CMP RM	ENH NP RM	normal_cm_enh	normal_np_enh
HETERO	HYPODENSE	ILLDEFINED	ABSENT	RV/IVC NOT INVOLVED	PRESENT	TCC	TCC	34	117	87	145	32	89	76	PRESENT	57	44	83	111
HOMO	HYPODENSE	WELL DIFINED	ABSENT	RV/IVC NOT INVOLVED	ABSENT	RCC	RCC	32	124	86	134	35	97	65	PRESENT	62	30	92	102
HETERO	HYPODENSE	WELL DIFINED	ABSENT	RENAL VEIN	ABSENT	RCC	RCC	31	132	78	138	36	104	90	PRESENT	68	54	101	107
HETERO	ISODENSE	WELL DIFINED	ABSENT	RV/IVC NOT INVOLVED	ABSENT	INFECTION	INFECTION	28	98	85	140	24	26	27	ABSENT	2	3	70	112
HETERO	ISODENSE	ILLDEFINED	ABSENT	RENAL VEIN	ABSENT	RCC	RCC	36	104	98	167	33	112	78	PRESENT	79	45	68	131
HETERO	HYPODENSE	ILLDEFINED	ABSENT	RENAL VEIN	PRESENT	RCC	RCC	26	123	103	145	28	104	77	PRESENT	76	49	97	119
HETERO	HYPODENSE	ILLDEFINED	ABSENT	RV/IVC NOT INVOLVED	ABSENT	RCC	RCC	34	130	84	132	34	112	95	ABSENT	78	61	96	98
HETERO	HYPODENSE	ILLDEFINED	ABSENT	RV/IVC NOT INVOLVED	ABSENT	RCC	RCC	34	110	78	137	37	97	67	ABSENT	60	30	76	103
HETERO	HYPODENSE	WELL DIFINED	ABSENT	RV and IVC INVOLVED	ABSENT	RCC	RCC	30	92	81	143	35	94	67	ABSENT	59	32	62	113
HETERO	HYPODENSE	WELL DIFINED	ABSENT	RV/IVC NOT INVOLVED	ABSENT	AML	AML	24	117	77	136	-24	-21	-15	ABSENT	3	9	93	112
HETERO	HYPODENSE	ILLDEFINED	ABSENT	RV/IVC NOT INVOLVED	ABSENT	AML	AML	32	128	72	144	-22	-15	-12	ABSENT	7	10	96	112
HETERO	HYPODENSE	WELL DIFINED	ABSENT	RV/IVC NOT INVOLVED	ABSENT	AML	AML	25	140	78	132	-24	-22	-19	ABSENT	2	5	115	107
HOMO	HYPODENSE	WELL DIFINED	ABSENT	RV/IVC NOT INVOLVED	ABSENT	INFECTION	INFECTION	32	135	91	122	23	23	25	ABSENT	0	2	103	90
HOMO	HYPODENSE	WELL DIFINED	PERIPHERAL	RV/IVC NOT INVOLVED	ABSENT	BOSNIAK TYPE 2 CYST	BOSNIAK TYPE 2 CYST	31	146	88	150	16	15	16	ABSENT	-1	0	115	119
HOMO	HYPODENSE	WELL DIFINED	PERIPHERAL	RV/IVC NOT INVOLVED	ABSENT	BOSNIAK TYPE 2 CYST	BOSNIAK TYPE 2 CYST	36	127	76	146	14	18	18	ABSENT	4	4	91	110
HETERO	HYPODENSE	ILLDEFINED	ABSENT	RV/IVC NOT INVOLVED	ABSENT	INFECTION	INFECTION	34	145	72	134	22	24	23	ABSENT	2	1	111	100
HOMO	HYPODENSE	WELL DIFINED	ABSENT	RV/IVC NOT INVOLVED	ABSENT	INFECTION	INFECTION	28	134	84	156	25	26	24	ABSENT	1	-1	106	128
HOMO	HYPODENSE	WELL DIFINED	ABSENT	RV/IVC NOT INVOLVED	ABSENT	INFECTION	INFECTION	25	154	84	145	20	21	24	ABSENT	1	4	129	120
HOMO	HYPODENSE	WELL DIFINED	PERIPHERAL	RV/IVC NOT INVOLVED	ABSENT	INFECTION	INFECTION	35	115	76	134	21	23	23	ABSENT	2	2	80	99
HETERO	HYPODENSE	WELL DIFINED	PERIPHERAL	RV/IVC NOT INVOLVED	ABSENT	AML	AML	36	124	73	143	-21	-20	-20	ABSENT	1	1	88	107
HETERO	HYPODENSE	WELL DIFINED	ABSENT	RV/IVC NOT INVOLVED	ABSENT	RCC	RCC	37	134	71	132	34	112	67	ABSENT	78	33	97	95
HETERO	HYPODENSE	ILLDEFINED	ABSENT	RV/IVC NOT INVOLVED	ABSENT	RCC	RCC	38	107	72	122	35	89	56	ABSENT	54	21	69	84
HETERO	HYPODENSE	ILLDEFINED	ABSENT	RENAL VEIN	ABSENT	RCC	RCC	31	101	67	134	33	78	70	ABSENT	45	37	70	103
HETERO	HYPODENSE	WELL DIFINED	ABSENT	RV/IVC NOT INVOLVED	ABSENT	RCC	RCC	34	123	66	132	36	98	64	ABSENT	62	28	89	98
HETERO	HYPODENSE	WELL DIFINED	ABSENT	RV/IVC NOT INVOLVED	ABSENT	INFECTION	INFECTION	35	108	68	132	22	23	23	ABSENT	1	1	73	97
HETERO	ISODENSE	WELL DIFINED	ABSENT	RV/IVC NOT INVOLVED	ABSENT	BOSNIAK TYPE III	BOSNIAK TYPE III	36	135	78	135	18	54	60	ABSENT	36	42	99	99
HOMO	HYPERDENSE	WELL DIFINED	ABSENT	RV/IVC NOT INVOLVED	ABSENT	RCC	RENAL METASTASIS	32	108	68	133	45	65	79		20	34	76	101
HETERO	HYPODENSE	ILLDEFINED	ABSENT	RV/IVC NOT INVOLVED	ABSENT	BOSNIAK TYPE IV	RCC	36	128	72	128	34	104	76	ABSENT	70	42	92	92
HETERO	HYPODENSE	WELL DIFINED	ABSENT	RV/IVC NOT INVOLVED	ABSENT	BOSNIAK TYPE IV	RCC	31	125	72	140	36	93	67	ABSENT	57	31	94	109
HOMO	HYPODENSE	WELL DIFINED	ABSENT	RV/IVC NOT INVOLVED	PRESENT	ONCOCYTOMA	ONCOCYTOMA	29	110	78	123	34	78	89	ABSENT	44	55	81	94